

國立交通大學

電子工程學系 電子研究所碩士班

碩士論文

二氧化鋯感測層在 N 型及 P 型 pH-離子感測場效電晶體上之
研究與比較

**The study and comparison of ZrO₂ sensing film based on
N-type and P-type pH-ISFETs**



學生：林佳鴻

Student: Chia-Hung Lin

指導教授：張國明 博士

Advisor: Dr. Kow-Ming Chang

桂正楣 博士

Dr. Cheng-May Kwei

中華民國九十六年七月

二氧化鋯感測層在 N 型及 P 型 pH-離子感測場效電晶體上之
研究與比較

**The study and comparison of ZrO₂ sensing film based on
N-type and P-type pH-ISFETs**

學生：林佳鴻

Student: Chia-Hung Lin

指導教授：張國明 博士

Advisor: Dr. Kow-Ming Chang

桂正楣 博士

Dr. Cheng-May Kwei



電子工程學系 電子研究所碩士班

碩 士 論 文

A Thesis

Submitted to Department of Electronics Engineering & Institute of
Electronics College of Electrical and Computer Engineering

National Chiao Tung University

In Partial Fulfillment of the Requirements

For the Degree of

Master

In

Electronics Engineering

July 2007

Hsinchu, Taiwan, Republic of China

中華民國九十六年七月

二氧化鋯感測層在 N 型及 P 型 pH-離子感測場效電晶體上之 研究與比較

學生：林佳鴻

指導教授：張國明 博士

桂正楣 博士

國立交通大學

電子工程學系 電子研究所碩士班



就我們所知離子感測場效電晶體(ISFET)是生物感測器的一種，它是利用浸泡在溶液中再去偵測其 pH 值，許多論文已經指出在長時間的操作下會有“漂移”現象的產生，“漂移”正如其名，就是閘極電壓在固定的電流下隨著時間會變動，當我們在量測的時候這種效性可能會造成其量測誤差，我們發現再“漂移”之後 pH-ISFET 的靈敏度會有變化，這是因為“漂移”所造成的，此效應便成了阻礙這產品再應用上的發展。

於本論文我們提出了一個方法去消除“漂移”這效應，我們發現“漂移”和溶液的 pH 值有一定的關係，然而“漂移”對於 N 型和 P 型 pH-ISFET 所表現的特性是相反的，基於這個原因我們可以透過電路利用這不同的效應去做補償而且補償之後的靈敏度會變成 N 型和 P 型 pH-ISFET 的平均，透過這種方法我們可以將“漂

移”變成一個定值不管經過多少時間或是用任何的 pH 溶液。為了實現這個想法，我們選用二氧化鋯去當 N 型和 P 型 ISFET 的感測層是基於它的高靈敏度，實驗的結果表示可以把“漂移”變成接近-26mV 的定值，它可以看成 pH-ISFET 的初始點的位移，這樣子就更容易補償透過其他電路方式，這種方法的優點在於不但可以消除“漂移”現象也可以維持高的靈敏度。

此外磁滯現象也會影響 pH-ISFET 的準確性，所以在本論文我們也會去討論此效應，我們選用二氧化鋯去當 pH-ISFET 的感測層，在實驗中發現它具有良好的磁滯特性，其最大的誤差大概是 0.111pH 值，所以我們可以知道二氧化鋯在 pH-ISFET 上是種很實用的材料。




The study and comparison of ZrO₂ sensing film based on N-type and P-type pH-ISFETs

Student: Chia-Hung Lin

Advisor: Dr. Kow-Ming Chang
Dr. Cheng-May Kwei

Department of Electronics Engineering & Institute of Electronics
National Chiao Tung University

ABSTRACT



So far as we know, the ion-sensitive field effect transistor (ISFET) is a kind of biosensor which via immersed the aqueous solution to detect the pH value. Some papers have already reported that at the long-term operation will cause a detrimental effect “Drift”. According to the meaning of “Drift” is that V_G shifts a value with time under the fixed current. The effect may cause the pH-ISFET inaccurately while measuring. We have already found the sensitivity of pH-ISFET variants after “Drift”, this situation is caused by “Drift”. The effect is one of the main reasons to obstruct the development of application.

In this study we propose a method to eliminate the “Drift”, we find that the “Drift” relates to the different pH value of aqueous solution. The “Drift” reveal opposite characteristic to N-type and P-type pH-ISFET, to base on the situation we can compensate this effect through the circuit and the sensitivity to pH-ISFET become the average sensitivity of N-type and P-type pH-ISFETs, and then the “Drift” can be

held to be a constant no matter how much time or any pH value of aqueous solution. To realize the idea, we prepare the ZrO_2 sensing film due to its high sensitivity which is based on the N-type and P-type pH-ISFETs. The results show that the “Drift” can be held nearly -26mV to any pH value aqueous for 6 hours, it can seem the offset of pH-ISFETs, and however it is more easily to compensate the offset through the other circuit. The advantages of this method are the elimination of “Drift” and keep the high sensitivity.

The hysteresis also causes the inaccuracy of pH-ISFETs, in our study we also discuss the effect to the pH-ISFET. It shows a good hysteresis characteristic to ZrO_2 based pH-ISFET from the results; its maximum error is 0.111pH value. It appears the ZrO_2 is a useful material to the pH-ISFET.



誌 謝

學生能完成此一論文，首先要感謝張國明老師以及桂正楣老師能讓我有機會參與 ISFET 的研究，張老師像慈父一般，桂老師像慈母一般不只在學術上給予我指導，也經常分享自己人生經驗給我，使我在交大不只學習到專業上的知識，更學習到做人的道理，在交通大學擁有最豐富的資源以及良好的研究環境，使我能夠順利完成論文。張老師和桂老師對於學生的關心以及照顧，讓我在忙碌研究生生活中，得到莫大的激勵，對我來說張老師和桂老師是我今生都不會忘記的恩師；也感謝龔正教授跟鄭兆禎博士給予的指點以及寶貴的意見讓我論文更完善。

其次要感謝張知天學長以及趙高毅學長對此論文實驗部分的完善規劃，以及在研究過程中如遇到困惑，他們的指導總讓我迎刃而解，當我有觀念上的錯誤，必定適時的糾正我，使我不再發生同的錯誤，這也使得研究能夠順利進行並且達到預期的實驗成果。

另外我還要感謝庭暉學長、信佑學長、同儕敬崑、智仁以及明聰學弟在實驗製程上的幫助，當實驗遇到困難時，總會互相討論於教學相長之下，使自己獲益良多得以順利的完成實驗；感謝宜軒在我心情鬱悶的時候總是會鼓勵我，使我的態度由消極轉為積極；還有感謝知天學長在歷次的討論當中所提出來意見對我都是很有建設性的幫助，讓我得以了解 ISFET 的基本架構以及內涵。

最後還要感養育我的父親林源榮先生，以及母親鄧保貴女士，由於兩位契而不捨的栽培，小兒才能完成現在的學業，他們不管自己多辛苦，總是會不計較的付出，很感謝兩位的支持，將來期許自己能夠為社會貢獻自己微薄的力量，不枉費老師以及父母對我的期許。

誌于 2007.07 林佳鴻

Contents

Abstract (in Chinese)	i
Abstract (in English)	iii
Acknowledgement	v
Contents	vi
Figure Captions	viii
Table Captions	xi
Chapter 1	Introduction 1
1.1	Brief history of ISFET..... 1
1.2	The evolution of the double layer models..... 1
1.2.1	The Helmholtz theory..... 2
1.2.2	The Gouy – Chapman theory..... 3
1.2.3	The Gouy – Chapman - Stern theory..... 3
1.3	Introduction to ISFET..... 4
1.4	Motivation of this work..... 5
1.5	References..... 6
Chapter 2	Theory & Drift Mechanism Description 9
2.1	Introduction..... 9
2.2	Why is pH important?..... 9
2.3	Definition of pH..... 10
2.4	The method for pH detection..... 10
2.5	The theory of ISFET..... 11
2.5.1	From MOSFET to ISFET..... 12
2.5.2	The Response of pH at the Oxide-Electrolyte Interface..... 14
2.6	Drift Phenomenon..... 16
2.6.1	Dispersive Transport..... 18

2.6.2	Expression for Drift.....	19
2.7	References.....	21
Chapter 3	Experiment and Measurement.....	24
3.1	Introduction.....	24
3.2	Fabrication Process.....	24
3.3	The key steps of the experiment.....	25
3.3.1	Gate region formation.....	26
3.3.2	Sensing layers deposition.....	26
3.4	Measurement system.....	27
3.4.1	Preparation of measurement.....	27
3.4.2	Current-Voltage measurement set-up.....	27
3.4.3	Drift measurement set-up.....	28
3.4.4	Hysteresis measurement set-up.....	29
3.5	References.....	29
Chapter 4	Results and Discussions.....	30
4.1	Introduction.....	30
4.2	The comparison with original sensitivity and after drift.....	30
4.3	The drift phenomenon to different pH aqueous solution.....	31
4.4	The influence on the hysteresis to the pH-ISFET.....	33
4.5	Conclusions.....	34
4.6	References.....	35
Chapter 5	Future Work.....	37
5.1	Future work.....	37

Figure captions

- Figure 1-1 Schematic representation of the side-binding model
- Figure 1-2 Schematic representation of the Helmholtz double layer model (a) The charge distribution (b) The potential distribution
- Figure 1-3 Schematic representation of Gouy and Chapman model (a)The charge distribution (b) The potential distribution
- Figure 1-4 Schematic representation of Gouy – Chapman – Stern model (a) The charge distribution (b) The potential distribution
- Figure 2-1 Schematic representation of (a) MOSFET, (b) ISFET
- Figure 2-2 Potential profile and charge distribution at an oxide electrolyte solution interface
- Figure 2-3 Series combination of the (a) initial (b) hydrated insulator capacitance
- Figure 3-1 Fabrication process flow
- Figure 3-2 Measurement setup
- Figure 3-3 Detection principle of pH
- Figure 3-4 Detection principle of drift
- Figure 4-1 I_d - V_g curve of ZrO_2 to n-type ISFET before drift
- Figure 4-2 Sensitivity characteristic of ZrO_2 to n-type ISFET before drift
- Figure 4-3 I_d - V_g curve of ZrO_2 to p-type ISFET before drift
- Figure 4-4 Sensitivity characteristic of ZrO_2 for p-type ISFET before drift
- Figure 4-5 I_d - V_g curve of ZrO_2 to n-type ISFET after drift in pH7 buffer solution for 7 hours
- Figure 4-6 Sensitivity characteristic of ZrO_2 to n-type ISFET after drift in pH7 buffer solution for 7 hours

- Figure 4-7 Id-Vg curve of ZrO₂ to p-type ISFET after drift in pH7 buffer solution for 7 hours
- Figure 4-8 Sensitivity characteristic of ZrO₂ to p-type ISFET after drift in pH7 buffer solution for 7 hours
- Figure 4-9 Sensitivity characteristic of ZrO₂ to n-type ISFET after drift in pH7 buffer solution 7 hours whose operation current is the same as original sensitivity
- Figure 4-10 Sensitivity characteristic of ZrO₂ to p-type ISFET after drift in pH7 buffer solution 7 hours whose operation current is the same as original sensitivity
- Figure 4-11 Time to drift in pH3 buffer solution of n-type ISFEET for 7 hours
- Figure 4-12 Time to drift in pH5 buffer solution of n-type ISFEET for 7 hours
- Figure 4-13 Time to drift in pH7 buffer solution of n-type ISFEET for 7 hours
- Figure 4-14 Time to drift in pH9 buffer solution of n-type ISFEET for 7 hours
- Figure 4-15 Time to drift in pH11 buffer solution of n-type ISFEET for 7 hours
- Figure 4-16 Time to drift rate of n-type ISFET in various buffer solution
- Figure 4-17 Time to drift in pH3 buffer solution of p-type ISFEET for 7 hours
- Figure 4-18 Time to drift in pH5 buffer solution of p-type ISFEET for 7 hours
- Figure 4-19 Time to drift in pH7 buffer solution of p-type ISFEET for 7 hours
- Figure 4-20 Time to drift in pH9 buffer solution of p-type ISFEET for 7 hours
- Figure 4-21 Time to drift in pH11 buffer solution of p-type ISFEET for 7 hours
- Figure 4-22 Time to drift rate of p-type ISFET in various buffer solution
- Figure 4-23 Time to drift of the compensation on the pH-ISFET in various buffer solution
- Figure 4-24 Time to drift rate of the compensation on the pH-ISFET in various buffer solution

- Figure 4-25 The comparison of drift between compensative drift and the original drift to the pH-ISFET in various buffer solution
- Figure 4-26 The comparison of sensitivity between compensative sensitivity and the original sensitivity to the pH-ISFET
- Figure 4-27 Hysteresis phenomenon to time of n-type pH-ISFET
- Figure 4-28 Hysteresis phenomenon to time of p-type pH-ISFET
- Figure 4-29 Hysteresis phenomenon to time of n-type pH-ISFET after drift in pH7 buffer solution for 7 hours
- Figure 4-30 Hysteresis phenomenon to time of p-type pH-ISFET after drift in pH7 buffer solution for 7 hours



Table captions

Table 3-1	(a) Specifications of wafers (b) Specifications of wafers Parameters of sensing layers deposition with Sputter
Table 4-1	Sensitivity at the optimum operation current
Table 4-2	Sensitivity at the immobile operation current
Table 4-3	Total drift in different pH buffer solution for 6 hours
Table 4-4	Drift rate in different pH buffer solution for 6 hours
Table 4-5	The comparison of the sensitivity
Table 4-6	The comparison of the sensitivity



Chapter 1

Introduction

1.1 Brief history of ISFET

In general, the application of sensors contains a widespread range including electrical, magnetic, physical, optical, thermal, and chemical...etc. The pH sensors belong to the category of 'chemical sensors'. The concept of the chemical sensor was first introduced in 1962 by the late Professor Kiyoyama of Kyushu University. Work in the field of FET chemical sensors began ten years after the discovery of the gas sensor.

Ion-sensitive field-effect transistors (ISFETs), first described by Bergveld in the early 1970s[1], have experienced a strong development. Bergveld describe the details of measurement of ion density with an ISFET-only configuration without a reference electrode. The operational mechanism of the ISFET with I_D , as an expression for the drain current in the linear region, for this reason as changes in the drain current are attributed to changes in the electrostatic potential only. In 1971, Professor Matsuo [2-3] conducted research on a high-impedance circuit using an organic microelectrode with an FET which proposed a measurement system employing the reference electrode. In 1978, an ISFET on a silicon island isolated by a P-N junction and insulator was proposed [1]. The discovery of the planar ISFET has been a revolutionary development for researchers previously restricted by the need for an insulating coating on the silicon substrate.

1.2 The evolution of the double layer model to ISFET

Briefly after description the history of ISFET it was recognized that there is a direct relation between the sensitivity of the ISFET and the charging behavior of metal oxides, the metal oxides always are used to be the sensing films of the ISFET. For a long period, the site-binding model (also called site-dissociation model) developed by Yates [4] was used to describe the ISFET pH sensitivity [5]. The site-binding model, illustrated in Figure 1-1, is indicated that reactions can happen between protons (H^+) in the solution and the hydroxyl groups formed at the oxide-solution interface. At chapter 2 will briefly derived the intrinsic buffer capacity, β_s at the site-binding model which is the important factor of the ISFET sensitivity.

In colloid chemistry, there is no consensus about the correct physical interpretation of the experimental observation on metal oxide. However, the most supported model for the ISFET pH sensitivity, a combination of a double layer model with a model describes the adsorption of protons. This is approach will be used to develop a new, more general model for the ISFET sensitivity. This new model can in incorporate any combination of a double layer model and a charging mechanism described by surface reaction. The theoretical calculations are verified with some experimental results. At the double layer model there is another important factor to the ISFET sensitivity, the double layer capacitance C_s , also been briefly derived at chapter 2.

1.2.1 The Helmholtz theory

There are several models to describe the double layer capacitance. In 1850's, the double layer structure for the metal-electrolyte interface was first supported by Helmholtz. He took the double layer as a parallel capacitance, illustrated in Figure 1-2.(a), The Helmholtz layer is divided into two plane, one is inner Helmholtz plane

which is dehydrated ions immediately next to a surface and the other is outer Helmholtz plane at the center of a next layer of hydrated. The capacitance between the inner and outer Helmholtz plane is the double layer capacitance C_s which depend on the surface potential which is contributed by the ions of the aqueous solution. The double layer capacitance is not a constant which follow the concentration of electrolyte. In Fig. 1-2(b), we can obtain the relation between the surface potential and the bulk potential is linear. As the concentration of electrolyte is very high, the Helmholtz double layer model is suitable for use, otherwise it can not be applied. Consequently, the Helmholtz double layer model need to be amended.

1.2.2 The Gouy – Chapman theory

The Helmholtz double layer model only considered the electrostatics force but ignore the thermal motion among the ions, so that it can not explain the value of the double layer capacitance, and the relation between the surface potential and the concentration of electrolyte which depend on each other. In the beginning of twenty century Gouy and Chapman proposed independently the idea layer to interpret the capacitive behaviour of an electrode-electrolyte solution interface.

Gouy and Chapman thought it was impossible that the ions were fixed at the metal-electrolyte interface regularly. The electrostatics force among electrode and ions, besides there is also an molecular thermal motion effect on the ions that makes a part of ions disperse near the bulk solution. As a result, the Gouy and Chapman model [6] was proposed to adjust the Helmholtz double layer model, illustrated in Figure 1-3. The Gouy and Chapman model has a major drawback. The ions are considered as a point charges that can approach the surface arbitrarily close. This assumption causes unrealistic high concentrations of ions near the surface at high value of surface

potential. An adjustment to solve this problem was first suggested by Stern [7].

1.2.3 The Gouy – Chapman - Stern theory

In 1924, Stern obtained if the concentration of electrolyte was high that the Helmholtz double layer model could match the experiment, but the concentration of electrolyte was not high enough the Gouy and Chapman model was suitable to use. For this reason, Stern thought the double layer model should combine the Helmholtz double layer model with the Gouy and Chapman model, so that the new model could explain any concentration of electrolyte for the double layer. This new model is called the Gouy-Chapman-Stern model, shown in Figure 1-4 illustrates. The Gouy-Chapman-Stern model involves two parts:

(1) The front part is stern layer which obey the Helmholtz double layer, the thickness d from the metal-electrolyte interface is nearly to the electrolyte ions radius, the great part of ions are included in the Stern layer.

(2) The later part is diffuse layer which contain remnant electrolyte ions, the ions decay according to the Gouy and Chapman model in this layer. Like Gouy, Stern also ignore the dimension of the ions in the diffuse layer. The surface potential to the bulk solution is the sum of the stern layer and the diffuse layer, and the double layer capacitance is series connection by the stern capacitance and the diffuse capacitance.

1.3 Introduction to ISFET

ISFET was proposed by Bergveld more than 30 years ago, more than 600 papers appeared in these 30 years devoted on ISFETs and another 150 on related devices, such as EnzymeFETs (ENFETs), ImmunoFETs (IMFETs)...etc [8]. By the way , the

pH-ISFTE can be not only a chemical sensor but also a physical sensor [9]. The pH-ISFET can measure the flow-velocity, flow-direction and diffusion-coefficient, it is showed that ISFET can be a multi-senor.

The ISFET has advantages over than ion selective electrode (ISE), such as small size, low coat and robustness. Traditional chemical analysis can not be the usual instrument, because of the size and even the coat that can not be the personal chemical analysis. For this reason, some people think the the traditional chemical analysis will be replace with ISFET or related devices of ISFET. In spite of ISFET have proposed more 30 years, there are less product in the market, the main problem is that ISFET has only sensing layer in its gate region which contact the aqueous solution. By contrast, in a CMOS process poly-si electrode in the gate region is required to define the self-aligned source and drain regions for the MOS transistors. This means that specific processes or design structures must be used to fabricated the ISFETs in a CMOS process.

The fabrication of pH-sensitivity ISFET devices in an undefined two-metal commercial CMOS technology is reported by J.Bausells [10]. Even though, when the pH-sensitivity ISFET operate for a long time, the problem “drift” is always be there.

1.4 Motivation of this work

Some people find out the low-drift material of sensing layer or coat a pasaivation layer onto sensing layer can reduce the drift phenomenon. Even if the two ways at process that can reduce the drift phenomenon, but as immerse the different pH value of aqueous solution, the degree of drift is distinct. The drift phenomenon according to any pH aqueous solution can not be the same, as ISFET operate at any pH aqueous solution for a long time, the value of ΔV_G is distinct from any different aqueous

solution will make ISFET detect the pH value inaccurate. This phenomenon can not avoid, whether use low-drift sensing layer or passivation layer. It becomes another problem, in order to improve this problem we will suppose a method to make the ΔV_G to be a constant or nearly zero as immerse the different pH value of aqueous solution, so it is more easily to compensate the ΔV_G .

The p-type ISFET use sol-gel process to prepare the tin oxide (SnO_2) sensing membrane, it show that there is a good linear characteristic of drift from pH 1 to pH 9 [11]. I suppose that the n-type ISFET probably has the opposite drift characteristic from different pH aqueous solution to p-type ISFET. According to the dispersive transport model for drift [12], we can discover that the degree of ΔV_G is dependent on the total charge in the sensing film, the depletion charge and the inversion charge which are different from the silicon substrate. Therefore, we can integrate the n-type ISFET and p-type to into a complementary ISFET to eliminate the drift. In case the absolute slope value of drift to different aqueous solution for p-type ISFET and n-type ISFET is the same, we can through the common mode circuit to hold the ΔV_G to be a constant. Consequently, it is more easily to compensate for the drift through the circuit. We will use ZrO_2 for the sensing film to n-type and p-type ISFET which is grown by sputter. In order to compare with the drift to different aqueous solution, the process to the n-type and p-type ISFET almost similar to each other. Detailed experiment steps will be presented in chapter 3, and the results will be discussed in chapter 4.

1.5 References

- [1] P. Bergveld, "Development of an ion sensitive solid-state device for neurophysiological measurements", IEEE Trans.Biomed. Eng.,vol. BME-17, p.70,

1970.

[2] T. Matsuo and K.D. Wise, An integrated field-effect electrode for biopotential recording, IEEE Transactions on Bio-Medical Engineering 21 (1974) 485.

[3] T. Matsuo and M. Esashi, Method of ISFET fabrication, Sensors and Actuators 1 (1982) 77.

[4] D.E. Yates, S. Levine and T.W. Healy, Site-binding model of the electrical double layer at the oxide/water interface. J. Chem. Soc. Faraday Trans. I, 70 (1974). 1807-1818

[5] L. Bousse, N.F. De Rooij and P. Bergveld, IEEE Trans. Electron. Dev., ED-30 (1983) 1263-1270

[6] R.E.G. van Hal, J.C.T. Eijkel and P. Bergveld, A general model to describe the electrostatic potential at electrolyte oxide interfaces, Adv. Coll. Interf. Sci. **69** (1996) 31-62.

[7] O. Stern, Z. Elektrochem., 30 (1924) 508.

[8] P. Bergveld, "Thirty years of ISFETOLOGY What happened in the past 30 years and what may happen in the next 30 years" Sensors and Actuators B 88 (2003) 1-20

[9] Arshak Poghosian, Lars Berndsen, Michael J. Schöning, Chemical sensor as physical sensor: ISFET-based flow-velocity, Sensors and Actuators B 95 (2003) 384-390

[10] J. Bausells, J. Carrabina, A. Errachid, A. Merlos, Ion-sensitive field-effect transistors fabricated in a commercial MOS technology, Sensors and Actuators B 57 (1999) 56-62

[11] Jung Chuan Chou, Yii Fang Wang, Preparation and study on the drift and hysteresis properties of the tin oxide gate ISFET by the sol-gel method, Sensors and Actuators B 86 (2002) 58-62

[12] S. Jamasb, S.D. Collins and R.L. Smith, A physical model for threshold voltage

instability in Si_3N_4 -gate H^+ -sensitive FET's (pH ISFET's), IEEE Trans. Electron Devices **45** (1998) 1239-1245.

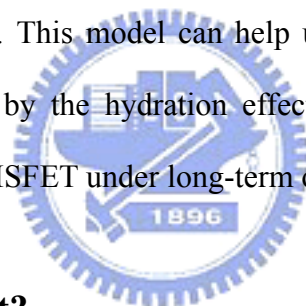


Chapter 2

Theory & Drift Mechanism Description

2.1 Introduction

In this chapter, pH, the theories of ISFET which are relevant to metal oxide semiconductor field effect transistor (MOSFET) and drift mechanism will be interpreted in turn. In the first section will describe what pH is briefly. Subsequently, the theory of ISFET include both ISFET concept and the relation between oxide to electrolyte interface. In the final section a physical model for drift developed by Jamasb [1] will be presented. This model can help us to understanding of the drift mechanism which is caused by the hydration effect and the ions transport in the insulater for the instability of ISFET under long-term operating.



2.2 Why is pH important?

Measuring pH is essential in finding the chemical characteristics of a substance. Thereinafter, these two examples can make us realize how important it is [2].

(1) Both the solubility of many chemicals or biomolecules in solution and the speed or rate of (bio-)chemical reactions are dependent on pH.

(2) The body fluid of living organisms usually has specific pH range. If the pH of the human blood changes by as little as 0.03 pH units or less the functioning of the body will be greatly impaired. The pH values of lakes, rivers, and oceans differ and depend on the kinds of animals and plants living there. All the industries that deal with water: from the drinking water, the food and the drugs to the paper, plastics,

semiconductors, cements, glass or textiles. In a word, pH is to be closely linked to us.

2.3 Definition of pH

The term pH is derived from a combination of p for the word power and H for the symbol of the element hydrogen [3]. In aqueous solution, the following equilibrium exists between the water (H₂O), the acid (H⁺) and the alkali (OH⁻):



pH is one of the most common chemical and biomedical measurements. The degree of the pH is the solution of ionization which can supply how much hydrogen ions (H⁺), not the concentration of the solution itself. The definition in pH is expressed as

$$pH = -\log a_{\text{H}^+} = -\log \gamma[\text{H}^+] \quad (2-2)$$

where a_{H^+} is the hydrogen ion activity, γ is the activity coefficient which equals to 1 when diluted solution, and $[\text{H}^+]$ is the molar concentration of solvated protons in units of moles per liter. In practice, pH depends on a number of factors, such as the concentration of the added acid and its dissociation constant [4].

2.4 The method for pH detection

Traditionally, the methods for the measurement of pH values include indicator reagent, pH test strips, metal electrode and glass electrode. There are some drawbacks on the other methods, except for glass electrode. Such as, indicator reagent can show different colors at different solvent, but it only exhibit a range of pH not the accuracy value; As pH test strips immersed in the test liquid, they show a particular color

corresponding to the pH of the solution. These are similar to indicator reagent; The hydrogen electrode method is a golden standard for all methods of pH measure. The activity of the hydrogen ions is determined by potentiometric measurement using a standard hydrogen electrode and a reference electrode. In order to ensure a saturated layer of hydrogen adsorbed at the platinum surface, hydrogen gas is continuously bubbled around the platinum electrode. However, this method is not suitable for daily use due to the inconvenience of handling hydrogen gas [2]. Because of some limitations in practical applications of the first three methods, the glass electrode becomes the most widely used method for the pH measurement, and it is considered to be the standard measuring method.

The glass electrode is most widely used for pH measurement due to ideal Nernstian response independent of redox interferences, short balancing time of electrical potential, high reproducibility and long lifetime. However, glass electrode has several drawbacks for many industrial applications. Firstly, they are unstable in alkaline or HF solutions or at temperatures higher than 100°C. Also, they exhibit a sluggish response and are difficult to miniaturize. Moreover, they cannot be used in food or in in vivo applications due to their brittle nature [1]. There is an increasing need for alternative pH electrodes [2].

New trends of pH measurements such as optical-fiber-based pH sensor, mass-sensitive pH sensor, metal oxide sensor, conducting polymer pH sensor, nano-constructed cantilever-based pH sensor, ISFET-based pH sensor and pH-imaging sensor. In this study, we will discuss what problems in practical applications of ISFETs and how to improve them.

2.5 The theory of ISFET

Since ISFET was the first reported by Bergveld, research on new material of sensing thin and fabrication process to improve the sensitivity and stability has been continuously proposed [5-7]. At the same time, the mechanism of the pH response of pH ISFET has also been studied extensively [6-12]. Electrochemical measurement of pH utilizes devices that transduce the chemical activity of the hydrogen ion into an electronic signal, such as an electrical potential difference or a change in electrical conductance. The followings are the theoretical foundations which are mostly adopted to characterize the ISFET.

2.5.1 From MOSFET to ISFET

The ISFET is a new approach of electrochemical measurement of pH, which is similar to MOSFET except that the metal/poly gate is replaced by sensing layers, and the sensing layer is immersed in aqueous solution. Because of it can not directly supply on the aqueous, therefore the reference electrode is adopted to connect with sensing layer. The reference electrode not only supply stable voltage but also can connect the circuit with sensing layer to make a loop. It can trace back to the history of the development of ISFET, it is not difficult to find out the similarities between ISFET and MOSFET. In general MOSFET is Metal-Insulator-Semiconductor structure, ISEFT is Electrolyte-Insulator-Semiconductor structure. The most obvious characteristic is the similarity between their structures. For this reason, the best way to comprehend the ISFET is to understand the operating principle of a MOSFET first.

When MOSFET is operated in the so-called ohmic or non-saturated region, the drain current I_D is given by:

$$I_D = \frac{C_{ox}\mu W}{L} \left\{ (V_{GS} - V_T) - \frac{1}{2} V_{DS} \right\} V_{DS} \quad (2-3)$$

where C_{OX} is the gate insulator capacitance per unit area; μ is the electron mobility in the channel; W/L is the width-to-length ratio of the channel; V_{GS} is gate to source voltage; V_{DS} is drain to source voltage and V_T is the threshold voltage. V_T can be described by following expression:

$$V_T = V_{FB} - \frac{Q_B}{C_{OX}} + 2\phi_F \quad (2-4)$$

where V_{FB} is the flat-band voltage; Q_B is the depletion charge in the silicon substrate, and ϕ_F is the potential difference between the Fermi level and intrinsic Fermi level.

The degree of ϕ_F is dependent on the doped concentration. V_{FB} can be described by following expression:

$$V_{FB} = \frac{\Phi_M - \Phi_{Si}}{q} - \frac{Q_{OX} + Q_{SS}}{C_{OX}} \quad (2-5)$$

where Φ_M is the work function of the gate metal; Φ_{Si} is the work function of silicon; Q_{OX} is the charge in the oxide and Q_{SS} is the surface state density at the oxide-silicon interface. Substitution of Eq. (2-4) in Eq (2-5), the general form of the threshold voltage of a MOSFET can be described by following expression:

$$V_T = \frac{\Phi_M - \Phi_{Si}}{q} - \frac{Q_{OX} + Q_{SS} + Q_B}{C_{OX}} + 2\phi_F \quad (2-6)$$

In the case of ISFET, the metallic gate is taken off. So that, the term Φ_M and Φ_{Si} are no longer to considered on the ISFET. At Figure 2-1 illustrates, it can observe the similarities and differences between MOSFET and ISFET. When immersed in a aqueous solution, it must occur surface potential at the oxide-solution interface. The surface potential must take in into account. Hence the threshold voltage become the following expression:

$$V_T = E_{ref} + \chi^{sol} - \Psi_0 - \frac{\Phi_{Si}}{q} - \frac{Q_{OX} + Q_{SS} + Q_B}{C_{OX}} + 2\phi_F \quad (2-7)$$

where E_{ref} is the constant potential of the reference electrode; χ^{sol} is the surface dipole potential of the solution which also has a constant value. The surface dipole

potential is different from aqueous solution, even though a little variation of surface dipole potential at disparity aqueous solution. The value compare to other term is too small to take as a constant. All terms are constant except Ψ_0 , it is the kernel of ISFET sensitivity to the electrolyte pH which is controlling the dissociation of the oxide surface. In order to obtain an accuracy pH value, to investigate a high pH sensitivity ISFET on the electrode-electrolyte interface is necessary.

2.5.2 The Response of pH at the Oxide-Electrolyte Interface

The surface of any metal oxide always contains hydroxyl groups, in the case of silicon dioxide SiOH groups [13]. These groups consist of donate and accept a proton from the solution. Therefore, as ISFET sensing layer like SiO₂ contact an aqueous solution, the change of pH will change the SiO₂ surface potential. These reactions can be expressed by:



where H_S^+ represents the protons at the surface of the oxide.

The potential between the gate insulator surface and the electrolyte solution causes a proton concentration difference between bulk and surface that is according to Boltzmann:

$$a_{H_S^+} = a_{H_B^+} \exp \frac{-q\Psi_0}{KT} \quad (2-10)$$

or

$$pH_S = pH_B + \frac{q\Psi_0}{2.3KT} \quad (2-11)$$

where a_{H^+} is the activity of H⁺; q is the elementary charge; k is the Boltzmann

constant and T is the absolute temperature. The subscripts B and S refer to the bulk and the surface, respectively.

There are two important parameters which are related to ISFET sensitivity, β_s and C_s . β_s is the symbol of the surface buffer capacity, the ability of β_s as the oxide surface to deliver or take up protons, and C_s is the differential double-layer capacitance, of which the value is mainly determined by the ion concentration of the bulk solution via the corresponding Debye length.

$$\frac{\Delta\sigma_0}{\Delta pH_s} = -q\beta_s \quad (2-12)$$

where σ_0 is the surface charge per unit area. β_s is called the intrinsic buffer capacity because it is the capability to buffer small changes in the surface pH (pH_s), but not in the bulk pH (pH_B).

Because of charge neutrality, an equal but opposite charge is built up in the electrolyte solution side of the double layer σ_{DL} , shown in Figure 2-2 illustrates. This charge can be described as a function of the integral double layer capacitance, C_i , and the electrostatic potential:

$$\sigma_{DL} = -C_i \Psi_0 = -\sigma_0 \quad (2-13)$$

The integral capacitance will be used later to calculate the total response of the ISFET on changes in pH. The ability of the electrolyte solution to adjust the amount of stored charge as result of a small change in the electrostatic potential is the differential capacitance, C_s :

$$\frac{\Delta\sigma_{DL}}{\Delta\Psi_0} = -\frac{\Delta\sigma_0}{\Delta\Psi_0} = -C_s \quad (2-14)$$

As a result, combination of Eq.(2-12) to (2-14) lead to an expression for the sensitivity of the the electrostatic potential change in a_{H^+} :

$$\frac{\Delta\Psi_0}{\Delta pH_s} = \frac{\Delta\Psi_0}{\Delta\sigma_0} \frac{\Delta\sigma_0}{\Delta pH_s} = \frac{-q\beta_s}{C_s} = \frac{\Delta\Psi_0}{\Delta(pH_B + \frac{q\Psi_0}{2.3KT})} \quad (2-15)$$

Rearrange Eq. 2-15 gives a general expression for the sensitivity of the electrostatic potential to changes in the bulk pH [13]:

$$\Delta\Psi_0 = -2.3\alpha \frac{kT}{q} \Delta pH_B \quad (2-16)$$

with

$$\alpha = \frac{1}{\frac{2.3kTC_s}{q^2\beta_s} + 1} \quad (2-17)$$

The parameter α is a dimensionless sensitivity parameter that varies between 0 and 1, depending on the intrinsic buffer capacity, β_s , of the oxide surface and the differential capacitance C_s . We can get the maximum value α so that the sensitivity become -59.2 mV/pH at 298K which is called Nernstian sensitivity. Therefore, the intrinsic buffer capacity β_s need to be the more higher or the double layer capacity C_s to be the more lower. In ideal, the intrinsic buffer capacity $\beta_s = \infty$ or the double layer capacity

$C_s = 0$ would be the best. It appears that the usual SiO_2 from MOSFET does not fulfil the requirements of a high vale of β_s . The pH sensitivity is low depending also on the electrolyte concentration through C_s . Therefore other films such as ZrO_2 were introduced to increase the values of β_s . The higher the intrinsic buffer capacity so that the less important of the value of C_s which means that independent of the electrolyte concentration a Nernstian sensitivity can be achieved over a pH range from 1 to 13.

2.6 Drift Phenomenon

Drift phenomenon is while ISFET expose to an aqueous solution for a long time, shift of ISFET gate voltage after a proper time from the response of the ISFET device. It has been reported by Dun et al. [18]. According to Hein and Egger [19], two types of drift have to be distinguished, the storage drift (irreversible shift without any applied voltages) and the long-term drift (irreversible shift under operating conditions). The initial drift means the drift after 3 h from the response starting [20]. The former's influence on drift is generally smaller than the latter. This result can be found in the previous work [1, 14-16] and also in the measurement data of this research. The phenomenon called drift is a slow, continuous, change of the threshold voltage of an ISFET in the same direction. It is difficult to identify the cause of this phenomenon, which could be either a surface or a bulk effect, or both. There are some possible reasons causes of drift [17].

(1) Variation of the surface state density (D_{it}) at the Si/SiO₂ interface which means the drift dependence of diffusion mechanism.

(2) Some surface effects, such as the rehydration of a surface that is partially dehydrated and ion exchange involving OH⁻ ions.

(3) Drift of sodium ion under the influence of the insulator field. Given an effective diffusion coefficient D_{eff} , it is clear that a bulk redistribution of sodium which has left a trap near the edge of the SiO₂.

(4) Injection of electrons from the electrolyte at strong anodic polarizations created negative space charge inside sensitive films.

Dun et al. [18] recognized that the drifts of Si₃N₄ and Ta₂O₅ gate ISFET both change toward the output voltage increasing. This condition is the same as that some negative charges (OH⁻) rise on the sensitive surface.

The great part of people most supported the drift phenomenon are the cases (1)

and (2). There are two models such as the site-binding model and the gel model, which are classified according to the location where the mechanism of pH-sensitivity is presumed to occur. These models can help us to have a further understanding of the transport of mobile ions. Nonetheless, these two models are only the characteristics of ions transport in the insulator, while the physical model for the gate voltage drift is going to be presented in the next section.

2.6.1 Dispersive Transport

Dispersive transport was briefly reviewed in [1] and it is observed in a broad class of disordered materials. In an amorphous material, dispersive transport may arise from hopping motion through localized states (hopping transport), trap-limited transport in the presence of traps possessing an exponential energy distribution (multiple-trap transport), or a combination of the aforementioned transport mechanisms (trap-controlled hopping transport) [21]. Regardless of the specific dispersive mechanism involved, however, dispersive transport leads to a characteristic power-law time decay of diffusivity [22] which can be described by

$$D(t) = D_{00} (\omega_0 t)^{\beta-1} \quad (2-18)$$

where D_{00} is a temperature-dependent diffusion coefficient which obeys an Arrhenius relationship, ω_0 is the hopping attempt frequency, and β is the dispersion parameter satisfying $0 < \beta < 1$. Dispersive transport leads to a decay in the density of sites/traps occupied by the species undergoing transport. This decay is described by the stretched-exponential time dependence given by

$$\Delta N_{S/T}(t) = \Delta N_{S/T}(0) \exp[-(t/\tau)^\beta] \quad (2-19)$$

where $\Delta N_{S/T}(t)$ is the area density (units of cm^{-2}) of sites/traps occupied, τ is the time

constant associated with structural relaxation, and β is the dispersion parameter.

2.6.2 Expression for Drift

In general, the surface of a sensing film is known to undergo a relatively slow conversion to a hydrated SiO_2 layer or contain oxygen atoms during contact with an aqueous solution [23-28]. Since hydration leads to a change of the chemical composition of the sensing film surface, it is reasonable to assume that the dielectric constant of the hydrated surface layer differs from that of the sensing film bulk. The overall insulator capacitance, which is determined by the series combination of the surface hydration layer and the underlying sensing film, will exhibit a slow, temporal change. When drift phenomenon occurs at the surface of an actively-biased ISFET, the gate voltage will simultaneously exhibit a change to keep a constant drain current.

The change in the gate voltage can be written as:

$$\Delta V_G(t) = V_G(t) - V_G(0) \quad (2-20)$$

Since the voltage drop inside of the semiconductor is kept constant, $\Delta V_G(t)$ becomes

$$\Delta V_G(t) = [V_{FB}(t) - V_{FB}(0)] + [V_{ins}(t) - V_{ins}(0)] \quad (2-21)$$

where V_{FB} is the flatband voltage and V_{ins} is the voltage drop across the insulator. V_{FB} and V_{ins} are given by the following expression:

$$V_{FB} = E_{ref} + \chi^{sol} - \Psi_0 - \frac{\Phi_{Si}}{q} - \frac{Q_{OX} + Q_{SS}}{C_{OX}} \quad (2-22)$$

$$V_{ins} = \frac{-(Q_B + Q_{inv})}{C_{OX}} \quad (2-23)$$

where Q_{inv} is the inversion charge. If the temperature, pH, and the ionic strength of the solution are held constant, E_{ref} , χ^{sol} , Ψ_0 , and Φ_{Si} can be neglected, so the drift can be rewritten as:

$$\Delta V_G(t) = -(Q_{OX} + Q_{SS} + Q_B + Q_{inv}) \left[\frac{1}{C_i(t)} - \frac{1}{C_i(0)} \right] \quad (2-24)$$

In this study, the gate oxide of the fabricated ISFET was composed of two layers, a lower layer of thermally-grown SiO₂ of thickness, x_L , and an upper layer of sputter-grown ZrO₂ of thickness, x_U . $C_i(0)$ is the effective insulator capacitance given by the series combination of the thermally-grown SiO₂ capacitance, ϵ_L/x_L , and the sputter-grown ZrO₂ capacitance, ϵ_U/x_U . $C_i(t)$ is analogous to $C_i(0)$, but an additional hydrated layer of capacitance make C_i always smaller than C_i , ϵ_{HL}/x_{HL} , at the oxide-electrolyte interface must be considered, and the sputter-grown ZrO₂ capacitance is now given by $\epsilon_U/[x_U - x_{HL}]$. The series combinations of the capacitances are illustrated in Figure 2-3. Therefore, the drift is given by

$$\Delta V_G(t) = -(Q_{OX} + Q_{SS} + Q_B + Q_{inv}) \left(\frac{\epsilon_U - \epsilon_{HL}}{\epsilon_U \epsilon_{HL}} \right) x_{HL}(t) \quad (2-25)$$

From this equation, we observed that drift of gate voltage ΔV_G if the substrate type was different, it might to be positive or negative value. Because of the value of ΔV_G is positive or negative, it is depend on the Q_{inv} and Q_B . Other terms at Eq.(2-25) can be appropriate as constant value no matter what the substrate is. According to this assume it is possible to eliminate the drift or hold the drift to be a constant at any other pH aqueous solution through the CMOS ISFET. By applying dispersive transport theory, an expression for $x_{HL}(t)$ is given by [1]

$$x_{HL}(t) = x_{HL}(\infty) \{1 - \exp[-(t/\tau)^\beta]\} \quad (2-26)$$

with

$$x_{HL}(\infty) = \frac{D_{00} \omega_0^{\beta-1} \Delta N_{S/T}(0)}{A_D \beta N_{hydr}} \quad (2-27)$$

where A_D is the cross-sectional area, and N_{hydr} is the average density of the hydrating species per unit volume of hydration layer. Thus, combination of Eq.(2-20) to (2-27) the gate voltage drift can be expressed by the following formula:

$$\Delta V_G(t) = -(Q_{OX} + Q_{SS} + Q_B + Q_{inv}) \left(\frac{\epsilon_U - \epsilon_{HL}}{\epsilon_U \epsilon_{HL}} \right) x_{HL}(\infty) \{1 - \exp[-(t/\tau)^\beta]\} \quad (2-28)$$

From this equation, we can expect that if the time of gate oxide immersing in the test-solution is long enough (determined by the constant τ), the gate voltage drift will approach a constant value which is greatly dependent on the hydration depth, $x_{HL}(\infty)$.

2.7 References

- [1] S. Jamasb, S.D. Collins and R.L. Smith, A physical model for threshold voltage instability in Si₃N₄-gate H⁺-sensitive FET's (pH ISFET's), IEEE Trans. Electron Devices **45** (1998) 1239-1245.
- [2] Y. Q. Miao, J. R. Chen and K. M. Fang, New technology for the detection of pH, J. Biochem. Biophys. Methods **63** (2005) 1-9.
- [3] Sfrenson SPL. Enzyme studies II: the measurement and meaning of hydrogen ion concentration in enzymatic processes. Biochem Z 1909;21:131–200.
- [4] D.A. Skoog, D.M. West, and F.J. Holler, Fundamentals of Analytical Chemistry, 7th ed., Philadelphia, PA: Saunders College Publishing, 1996.
- [5] Tadayuki Matsuo and Masayoshi Esashi, Methods of ISFET fabrication, Sens. Actuators **1** (1981) 77-96.
- [6] Massimo Grattarola and Giuseppe Massobrio, Bioelectronics handbook: MOSFETs, biosensors, and neurons, McGraw-Hill, New York, 1998.
- [7] P. Bergveld, "Thirty years of ISFETOLOGY What happened in the past 30 years and what may happen in the next 30 years" Sensors and Actautors B 88 (2003)1-20
- [8] Wouter Olthuis, Chemical and physical FET-based sensors or variations on an equation, Sens. Actuators B **105** (2005) 96-103.

- [9] D.E. Yates, S. Levine and T.W. Healy, Site-binding model of the electrical double layer at the oxide/water interface, *J. Chem. Soc., Faraday Trans.* **70** (1974) 1807-1818.
- [10] Luc Bousse, Nico F. de Rooij and P. Bergveld, Operation of chemically sensitive field-effect sensors as a function of the insulator-electrolyte interface, *IEEE Trans. Electron Devices* **ED-30** (1983) 1263-1270.
- [11] R.E.G. van Hal, J.C.T. Eijkel and P. Bergveld, A novel description of ISFET sensitivity with the buffer capacity and double-layer capacitance as key parameters, *Sens. Actuators B* **24-25** (1995) 201-205.
- [12] R.E.G. van Hal, J.C.T. Eijkel and P. Bergveld, A general model to describe the electrostatic potential at electrolyte oxide interfaces, *Adv. Coll. Interf. Sci.* **69** (1996) 31-62.
- [13] Dr. Ir. P. Bergveld Em University of Twente, ISFET, Theory and Practice, IEEE sensor conference Toronto, October 2003 1-26.
- [14] S. Jamasb, S. Collins and R.L. Smith, A physically-based model for drift in Al₂O₃-gate pH ISFET's, *Tech. Digest, 9th Int. Conf. Solid-State Sensors and Actuators (Transducers '97)*, Chicago, IL, 15-19 June, 1997, 1379-1382.
- [15] S. Jamasb, S. Collins and R.L. Smith, A physical model for drift in pH ISFETs, *Sens. Actuators B* **49** (1998) 146-155.
- [16] S. Jamasb, An analytical technique for counteracting drift in Ion-Selective Field Effect Transistors (ISFETs), *IEEE Sens. J.* **4** (2004) 795-801.
- [17] Luc Bousse and P. Bergveld, The role of buried OH sites in the response mechanism of inorganic-gate pH-sensitive ISFETs, *Sens. Actuators* **6** (1984) 67-78.
- [18] Yu Dun, Wang Guihua, Wu Shixiang, *Chin. J. Sensor Technol.* **5** (1991) 57.
- [19] Zhong Yule, Zhao Shouan, Lin Tao, *Chin. J. Semiconduct.* **15** (1994) 838.
- [20] Peter Hein, Peter Egger, Drift behaviour of ISFETs with Si₃N₄-SiO₂ gate

insulator, *Sensors Actuators B* 13-14 (1993) 655.

[21] G. Pfister and H. Scher, "Time-dependent electrical transport in amorphous solids: As₂Se₃," *Phys. Rev. B.*, vol. 15, no. 4, p. 2062, 1977.

[22] R. A. Street and K. A. Winer, "Defect equilibria in undoped a-Si:H," *Phys. Rev. B.*, vol. 40, no. 9, pp. 6236–6249, 1989.

[23] M. Esashi, and T. Matsuo, "Integrated micro multi ion sensor using field effect of semiconductor," *IEEE Trans. Biomed. Eng.*, vol. BME-25, pp. 184–192, Mar. 1978. *Devices*, vol. ED-26, p. 1805, Nov. 1979.

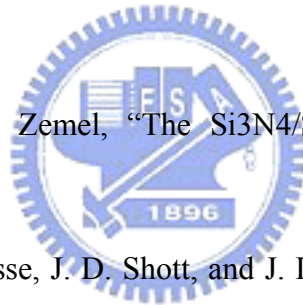
[24] H. Abe and T. Matsuo, "ISFET's using inorganic gate thin films," *IEEE Trans. Electron Devices*, vol. ED-26, p. 1939, Dec. 1979.

[25] T. Matsuo and M. Esashi, "Methods of ISFET fabrication," *Sens. Actuators*, vol. 1, pp. 77–96, 1981.

[26] I. R. Lauks and J. N. Zemel, "The Si₃N₄/Si ion-sensitive semiconductor electrode," *IEEE*.

[27] D. L. Harame, L. J. Bousse, J. D. Shott, and J. D. Meindl, "Ion-sensing devices with silicon nitride and borosilicate glass insulators," *IEEE Trans. Electron Devices*, vol. ED-34, pp. 1700–1707, Aug. 1987.

[28] P. Bergveld and A. Sibbald, in *Comprehensive Analytical Chemistry*, vol. XXIII. Amsterdam, The Netherlands: Elsevier, 1988.



Chapter 3

Experiment and Measurement

3.1 Introduction

ISFET has the same manufacturing process as the conventional MOSFET. The difference between MOSFET and ISFET procedure is the process of gate electrode. The ISFET take the gate membrane as a sensing layer immersed in the pH-solution [1], and the reference electrode is placed overhead the sensing layer as the gate voltage

controller. In theory, the sensitivity of n-type ISFET and p-type ISFET must be the same, the definition of sensitivity of ISFET is already interpreted at chapter 2. According the definition there is no any factor about electrons and holes, so that I speculate about the sensitivity must be the same whether the substrate is n-type or p-type. The drift and hysteresis are important factors that influence the output accuracy of the pH-ISFET. At chapter 4, the sensitivity after to ISFET, the different pH value to drift and the hysteresis will be discussed. The next section is the fabrication process flow of the n-type and p-type ISFET devices which are used for investigating the drift characteristics. Finally, the measurement setup, and the detection principles of pH and drift will be presented.

3.2 Fabrication Process

All procedures of experiment are done in NDL (National Nano Device Laboratory) and NFC (Nano Facility center), similar to the manufacturing process of

MOSFET [2]. The process flow of ISFET is illustrated in Figure 3-1. The sensing layers ZrO_2 is deposited onto the SiO_2 gate ISFET which prepared by Sputter in Nano Facility center. Before every step, besides after sensing membrane deposited onto SiO_2 gate, the initial clean immersed in $H_2SO_4+H_2O_2$ about 5 minutes and dipped in HF solution were done. The fabrication parameters are listed in Table 3-1(a), 3-1(b) and the fabrication procedures are listed as follows:

a) RCA clean

Wet-oxidation, 6000\AA , 1050°C

b) Defining of S/D (mask 1)

BOE wet-etching of SiO_2

c) Dry-oxidation, 300\AA , 1050°C

S/D ion implantation

($5e15$ ($1/\text{cm}^2$), 25Kev (Phosphorus) for n-type ISFET)

($5e15$ ($1/\text{cm}^2$), 15Kev (Boron) for p-type ISFET)

S/D annealing, 950°C , 60min

d) PECVD SiO_2 for passivation, $1\mu\text{m}$

e) Defining of contact hole and gate region (mask 2)

BOE wet-etching of SiO_2

f) Dry growth of gate oxide, 100\AA , 850°C

g) Sputtering ZrO_2 as sensing layer, 300\AA (mask 3)

ZrO_2 sintering, 600°C , 30min

h) Al evaporation, 5000\AA (mask 4)

Al sintering, 400°C , 30min

3.3 The key steps of the experiment

3.3.1 Gate region formation

RCA clean is usually performed at wafer starting to reduce the possible pollution such as particles, organics, diffusion ions and native oxide. Careful RCA clean will ensure the integrity of device electricity. The next step 600nm thickness wet oxide is deposited as barrier layer for S/D implant. The density and the energy of S/D implant is $5E15$ ($1/cm^2$) and 25Kev with phosphorous dopant for n-type ISFET, and $5E15$ ($1/cm^2$) and 15Kev with Boron for p-type ISFET. After S/D implanting, in order to activate the dopants, a $950^\circ C$ 30min N^+ anneal for n-type ISFET and a $950^\circ C$ 30min P^+ anneal are done.

The extra $1\ \mu m$ thickness PECVD oxide deposition is essential, which protect the other pH-ISFET from aqueous solution overflowing pH-ISFET [3]. During a long period of electrolyte immersing, ions may diffuse and affect the ISFET's electrical characterization [4]. It is a significant difference compare with standard MOSFET processes. A thick PECVD oxide deposition can eliminate the effect. Following the PECVD oxide deposition, 100\AA thickness dry oxide was grown in a dry oven as gate oxide formed.

3.3.2 Sensing layer deposition

This procedure is the kernel of the pH-ISFET in our important part in our experiment. The ZrO_2 sensing film 300\AA is growth by the sputter which appear a good sensitivity nearly Nernstian sensitivity [5]. The detailed parameters of sputter are listed in Table 3.1 (b).

3.4 Measurement system

3.4.1 Preparation of measurement

To investigate the characteristics of the ZrO_2 as sensing layers, we measured the I-V curves for the pH-ISFETs by using HP4156 as measurement tool and the system is shown in Fig. 3-2. For getting correct result of measurement, the entire measurement procedures were executed in a dark box to prevent light influence and the electromagnetic wave.

In order to make the sensing film immersed in the aqueous solution, some extra works on wafers must be done before measurement with HP4156. At first, we glued a container on the wafer. This step is very important for following complex and frequently solution change activities which also can protect the other ISFET from immersed aqueous solution. The container, to load the test electrolyte, was open at its bottom and covered the whole sensing region on wafer to keep electrolyte contact with sensing layers exactly.

The pH-standard solution is purchased by Riedel-deHaen corp. and the pH-values are 1,3,5,7,9,11,13. The electric potential of the pH-solution will be floating [6] during open-loop circuit. The disturbance from the environment would induce the electric potential variance of the solution. By eliminating this variance, a reference electrode is needed to immersion in the pH-solution to close the circuit loop.

3.4.2 Current-Voltage measurement set-up

A HP-4156 semiconductor parameter analyzer system were set up to measure the current-voltage (I-V) characteristics curves, in which included I_{ds} - V_{gs} and I_{ds} - V_{ds}

curves at controlled temperature. All measurements were arranged in a dark box to minimize the effects of photoelectric and temperature.

In the I-V measurements, due to the sensing areas were so small, prevention of air bubbles from being generated between the sensing membrane and the buffer solution during the testing is needed to take care.

In the setup of HP-4156, substrate voltage is ground to avoid the body effect and the reference electrode is sweeping to different voltage. In the measurement of sensitivity, the response of the pH-ISFET is the function of time. According to P. Woias [9], the first equilibrium will achieves in a minute.

In order to obtain the sensitivity, at first we measure the I_{ds} - V_{ds} to observed the linear area. Secondly, we make the V_{ds} as constant to measure I_{ds} - V_{ds} from pH 13 to pH1 in turn. As changing the pH buffer solution, we diluted next butter solution which under test twice, and stay 1min to avoid the effect of the buffet solution that measured before. This step can make our the measurement of pH-ISFET more easily. The variation of the gate voltage exhibits the pH sensitivity of the sensing oxide. Figure 3-3 illustrates the detection principle of pH

3.4.3 Drift measurement set-up

The drift characteristics were measured with differential pH value of aqueous solution and the same condition samples period of 30 seconds, 1 minute, 10 minutes and 1 hour. 33 sampling points in the time frame of 7 hours were observed for n-type and p-type ISFET with ZrO_2 . The detection principle is in a similar manner to that of the pH measurement and is shown in Figure 3-4.

3.4.4 Hysteresis measurement set-up

For characterizing the hysteresis phenomena of ISFETs, we measured I-V curves for etch film with changing the pH-solution in the order of pH 7-1-7-13-7-1-7-13, and back to pH 7. For each pH value we got 3 measure points with duration of 1 min, detailed dilute works were done before electrolytes changed.

3.5 References

- [1] P. Bergveld, "Thirty years of ISFETOLOGY What happened in the past 30 years and what may happen in the next 30 years" *Sensors and Actautors B* 88 (2003)1-20
- [2] T. Matsuo and M. Esashi, *Methods of ISFET fabrication*, *Sensor. & Actuator* 1 (1981) 77-96.
- [3] U. Guth, "Investigation of corrosion phenomena on chemical microsensors", *Electrochimica Acta* 47 pp. 201–210 , 2001.
- [4] George T. Yu, "Hydrogen ion diffusion coefficient of silicon nitride thin films", *Applied Surface Science* 202 pp.68–72, 2002.
- [5] K. M. Chang, K. Y. Chao, T. W. Chou, and C. T. Chang,"Characteristics of Zirconium Oxide Gate Ion-sensitive Field-Effect Transistors" *Japanese Journal of Applied Physics* Vol. 46 No. 7A pp. 4334-4338 2007.
- [6] P. Woias, "Slow pH response effects of silicon nitride ISFET sensors", *Sensors*

Chapter 4

Results and Discussions

4.1 Introduction

The drift is an inevitable phenomenon of pH-ISFETs, some studies already indicate that the gate voltage shift according to the immersed time goes on. In case of the sensitivity changed as the pH-ISFETs immersed the aqueous solution, it will make pH-ISFETs sensing ability inaccurate. Therefore, the original sensitivity of pH-ISFETs compare with the sensitivity after drift will discuss in the first section. Afterward the drift to different pH value of aqueous solution will be showed, in our mind we anticipate that the drift to different pH value aqueous solution to different type of substrate is opposite, which is proposed at the chapter1. We can compensate the drift to gate voltage if the idea established. At the last section we will discuss with the hysteresis to pH-ISFETs which make detection of pH value inaccuracy, to look into the effect cause the error to detection pH value whether it is acceptable for pH-ISFETs or not.

4.2 The comparison with original sensitivity and after drift

The pH sensitivity is one of the important characteristic parameters of ISFET devices and the response of an ISFET is mainly governed by the type of sensing materials, in order to gain the higher sensitivity the high-k material is needed to the pH-ISFETs. As a results we select the ZrO_2 as a sensing film of pH-ISFET, the sensitivity can nearly achieve the Nernstian sensitivity [1]. Figure 4-1 is the measured I_d - V_g curve from pH13 to pH1 of the n-type pH-ISFET, and Figure 4-2 is the

sensitivity of it. When calculating the sensitivity we always select the point of maximum g_m , because at this point the efficiency of amplifying signal is best. It shows high sensitivity 58.73mV/pH nearly Nernstian sensitivity 58.9mV/pH. Figure 4-3, 4-4 are the I_d - V_g curve and sensitivity of p-type pH-ISFET, it also show high sensitivity 57.8mV/pH, for this reason the difference between the n-type and p-type pH-ISFET is only the carrier not relate with the sensitivity. Figure 4-5, 4-6 show the I_d - V_g curve and sensitivity of n-type pH-ISFET after immersed in the pH7 buffer solution for 7 hours. We observe that the sensitivity less changed after drift for 7 hours, if the optimum operation point is the maximum g_m . The characteristic of ISFET is invariable even it immersed for 7 hours, but the optimum operation point shift as the time goes on. Figure 4-7, 4-8 is the I_d - V_g curve and sensitivity of p-type pH-ISFET after immersed in the pH7 buffer solution for 7 hours. The situation is the same as n-type pH-ISFET, it doesn't matter that pH-ISFET is n-type or p-type. The sensitivity compare with n-type and p-type at the optimum operation current after drift is showed at the Table 4-1, and at the immobile operation current is showed at the Table 4-2.

However, in fact the optimum operation point is fixed as the device produced. Figure 4-9 is the sensitivity of n-type ISFET after immersed in the pH7 buffer solution for 7 hours, but the current is the as before drift. We can discern that the operation point not mean the maximum g_m , the sensitivity change into 51.01mV/pH which is less 7.72mV/pH than original sensitivity. The influence on sensing pH value may cause the error of 0.13pH value; the lower sensitivity may cause the larger error for the pH-ISFET. The p-type ISFET has the same state which is showed in Figure 4-10. The reason caused the phenomenon will be discussed in next section.

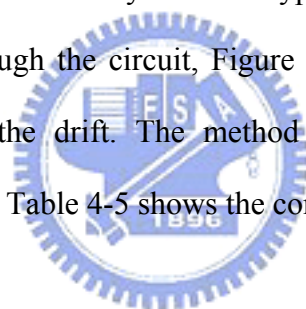
4.3 The drift phenomenon to different pH aqueous solution

The drift phenomenon has limited the commercial viability of ISFET based sensors by imposing special requirements for burn-in, packaging, and/or compensation. This phenomenon is a complex effect to pH-ISFET which relate to time, sensing film quality [2] and pH aqueous solution. In order to investigate the different pH aqueous solution to drift, the time and the film must be controlled at same condition. Figure 4-11~4-15 is the times for 7 hours drift in the pH 3, 5, 7, 9, 11 aqueous solution of n-type ISFET. From these illustrations we can perceive that the drift is a time dependent function which is studied by S. Jamasb [2], the drift for 7 hours is too short to reach the stable state. We can find that the drift is dependent on pH aqueous solution from figure 4-16, the drift rate is increasing with pH value. According to Bousse and Bergveld [3], the mechanism of injection into electrons from the electrolyte cause strong anodic polarizations created negative space charge inside sensitive films [4, 5]. The existence of OH^- ion is one of the factors that cause the drift [6]; OH^- ions which exist in the acid solutions are lesser than in alkaline solutions. According to this drift mechanism, we can find that for n-type ISFET the ΔV_T increase with the pH value which is due to the negative space charge inside sensitive films. The drift rate difference in the pH buffer solution is less than sol-gel SnO_2 oxide, but the drift magnitude compare with the sol-gel SnO_2 oxide is less in the same pH buffer solution. The main reason causes this situation which relate to the effective charge per unit area Q_f , time and the variation terms in Eq.(2-25) of ZrO_2 . For this reason we can know the various effect results in the drift that we mean.

Figure 4-17~4-21 show times for 7 hours drift in the pH 3, 5, 7, 9, 11 aqueous solution of p-type ISFET. However the drift is a complex factors effect, the reasons that we describe above front paragraph. As a result of the drift effect to pH-ISFET which use sensing film as ZrO_2 , the effect cause the OH^- ions increase with the pH

value. To p-type the OH^- ions increase may decrease threshold voltage, the situation is opposite to n-type pH-ISFET which is showed in Figure 4-22. The comparison of the total drift and drift rate to pH-ISFETs is showed at the table 4-3 and 4-4.

The drift reveals opposite influence on the n-type and p-type pH-ISFET, we can through the circuit to sum the effect to compensate the drift. Figure 4-23, 4-24 are the compensated drift and drift rate that we summed the different type of drift, and then divided by 2. We can observe that the compensation for the drift through the circuit compare with the n-type and p-type pH-ISFETs, it can make the drift to be nearly constant which is showed in the Figure 4-25. For this reason as the drift can be hold to be a constant, it is more easily to compensate the pH-ISFET. However the sensitivity becomes the average original sensitivity of the n-type and p-type pH-ISFETs while we compensate the drift through the circuit, Figure 4-26 shows the new sensitivity after the compensation for the drift. The method is easily to realize and have advantages for the pH-ISFET. Table 4-5 shows the comparison of the pH-ISFETs.

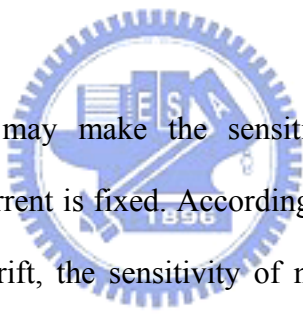


4.4 The influence on the hysteresis to the pH-ISFET

The hysteresis phenomenon may cause the pH-ISFET to sense the pH value inaccurately; the ΔV_G to n-type ISFET after the 1st cycle and the 2nd cycle is showed in the Figure 4-27. At the 1st cycle the hysteresis cause the ΔV_{G1} shift 5.61mV, this effect may make the 0.095pH value error and $\Delta V_{G2}=3.79\text{mV}$ makes the 0.064pH value error at the 2nd cycle to the n-type pH-ISFET. Figure 4-28 is the hysteresis to the p-type ISFET, at the 1st cycle $\Delta V_{G1}=6.33\text{mV}$ and $\Delta V_{G2}=2.18\text{mV}$ at 2nd cycle, it may cause the 0.111pH value error at 1st cycle and 0.038pH value error at pH value. The pH-ISFET based on sensing film ZrO_2 has a good characteristic of hysteresis to any type of pH-ISFET, the phenomenon causes the pH-ISFET sensor error is lower. Figure

4-29, 4-30 are the hysteresis to n-type and p-type pH-ISFET after drift in the pH7 buffer solution for 7 hours. The $\Delta V_{G1}=2.41\text{mV}$, and $\Delta V_{G2}=0.47\text{mV}$ to n-type pH-ISFET may cause the 0.043pH value error at 1st cycle and 0.0084pH value error at the 2nd cycle. To p-type pH-ISFET the $\Delta V_{G1}=4.95\text{mV}$ cause the 0.089pH value error, and $\Delta V_{G2}=1.63\text{mV}$ make 0.029pH value error. The hysteresis after drift in pH7 buffer solution for 7 hours is less than the pH-ISFET drift not yet. The hysteresis phenomenon includes the drift effect, the pH-ISFET is more stable after drift than before, and the situation to n-type and p-type pH-ISFET is the same. Table 4-6 is the comparison of hysteresis before and after drift to pH-ISFETs.

4.5 Conclusion



The drift phenomenon may make the sensitivity differ from the original sensitivity, if the operating current is fixed. According to the results, we can find that the sensitivity change after drift, the sensitivity of n-type pH-ISFET is lower than original sensitivity before but it is higher than original sensitivity to p-type pH-ISFET. The reason for this situation is the ΔV_G different from each other after drift, the drift magnitude is dependent on the effective charge per unit area Q_i , time and the variation terms in Eq.(2-25). At Figure 4-9, 4-10 we can observe that the n-type pH-ISFET driving current is less than p-type, the influence on the drift may make the gate voltage shift. The drift may cause the gate voltage shift, if the driving current is too small that the gate voltage may dominate it. According to the Eq.(2-3), to increase the driving current such as decrease channel length, increase the mobility or use high-k material to increase the capacitance, these way may decrease the influence on the drift to pH-ISFET. Therefore, the sensitivity can be held even after long-term drift.

The drift cause the variation of sensitivity, we also can use current to compensate

the drift effect. We propose the way of using the drift to the different pH value aqueous solution for different type of pH-ISFET, the state is opposite to different type of pH-ISFET. To sum the drift to different type of pH-ISFET in different aqueous solution, we get the nearly a constant -26mV of drift. It can seem the offset to the pH-ISFETs, however it is more easily to compensate the offset through the other circuit, the sensitivity also can be held through this method.. The advantages of the method: 1. No matter using any oxide for the pH-ISFET, it can improve the drift even it is not linear by the drift is opposite to different type of pH-ISFET: 2. The sensitivity is the average of two type of pH-ISFET, it can keep high sensitivity nearly 57.9mV/pH of ZrO₂ sensing film while through the method.

The ZrO₂ show a good characteristic of hysteresis to pH-ISFET, the effect only cause the maximum error of 0.095pH value on the n-type pH-ISFET, to p-type it cause error of 0.011pH value. The error can be accepted in the application by using the pH-ISFET. The hysteresis effect after drift is less than before, it reveals that the hysteresis includes the drift; the hysteresis to two type of pH-ISFET is more stable after drift.

4.6 References

- [1] K. M. Chang, K. Y. Chao, T. W. Chou, and C. T. Chang, "Characteristics of Zirconium Oxide Gate Ion-sensitive Field-Effect Transistors" Japanese Journal of Applied Physics Vol. 46 No. 7A pp. 4334-4338 2007.
- [2] S. Jamasb, S.D. Collins and R.L. Smith, A physical model for threshold voltage instability in Si₃N₄-gate H⁺-sensitive FET's (pH ISFET's), IEEE Trans. Electron Devices **45** (1998) 1239-1245.
- [3] L. Bousse, P. Bergveld, The role of buried OH⁻ sites in the response mechanism

of inorganic-gate pH-sensitive ISFETs, *Sens. Actuat.* 6 (1984) 65–78.

[4] L.Bousse and P.Bergveld, *J. Electroanal. Chem.*, 152 (1983) 25

[5] E. H. Nicollian, C. N. Berglund, P. F. Schmidt and J.M. Andrews, *J. Appl Phys.*, 42 (1971) 5654.

[6] Jung Chuan Chou, Yii Fang Wang, Preparation and study on the drift and hysteresis properties of the tin oxide gate ISFET by the sol–gel method, *Sensors and Actuators B* 86 (2002) 58–62

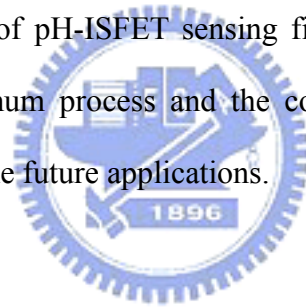


Chapter 5

Future Work

5.1 Future Work

In the study, the method of improving the drift has already experimented. Although we can make the drift be a constant by this method, but the constant is not zero. This situation is caused by the threshold voltage mismatch to n-type and p-type pH-ISFET. The threshold voltage can be adjusted by the ion implantation in, and then we must control the quality of pH-ISFET sensing film. Therefore, the drift can be eliminated through the optimum process and the compensative method, it will be suitable to the pH-ISFET in the future applications.



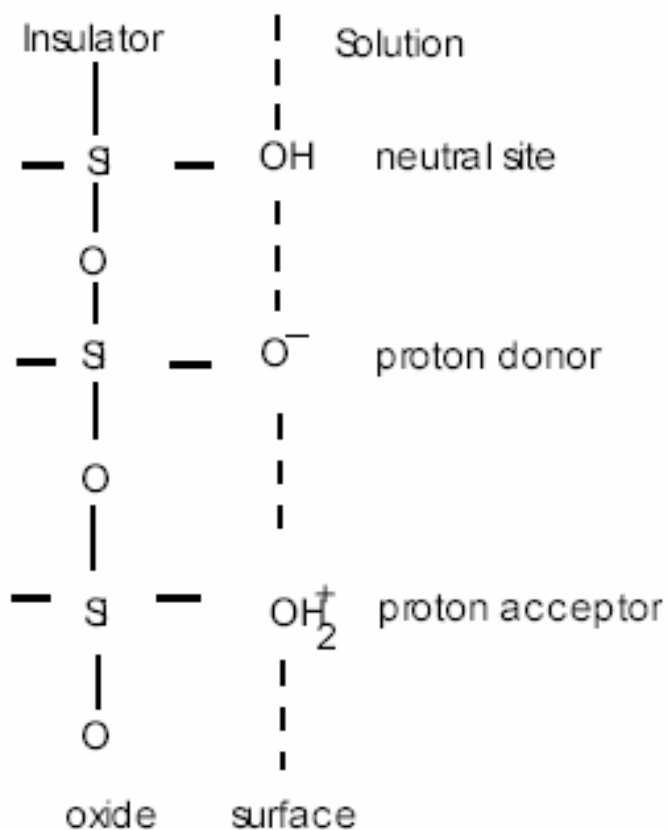


Figure 1-1 Schematic representation of the side-binding model

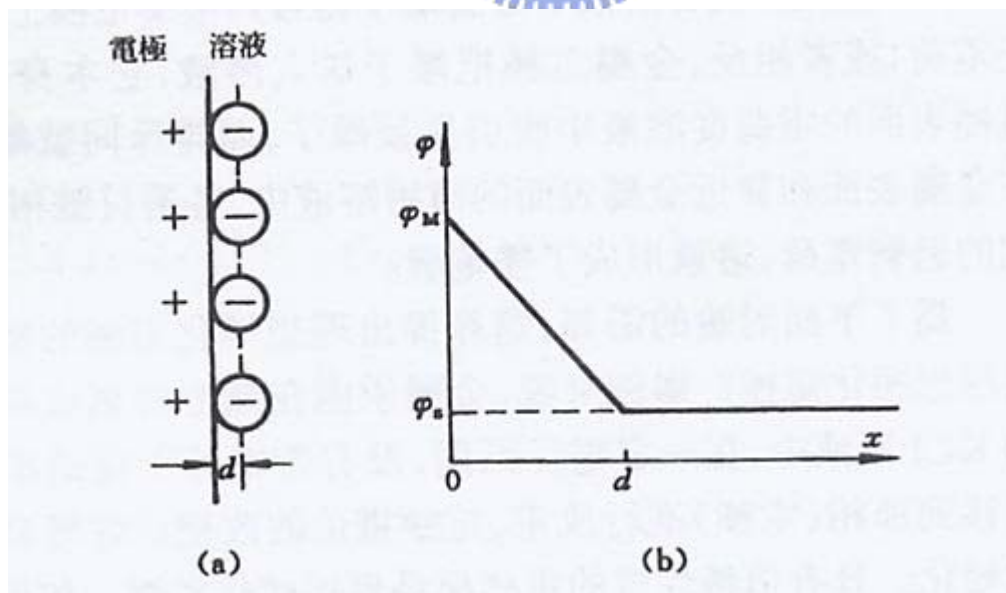


Figure 1-2 Schematic representation of the Helmholtz double layer model

(a) The charge distribution (b) The potential distribution

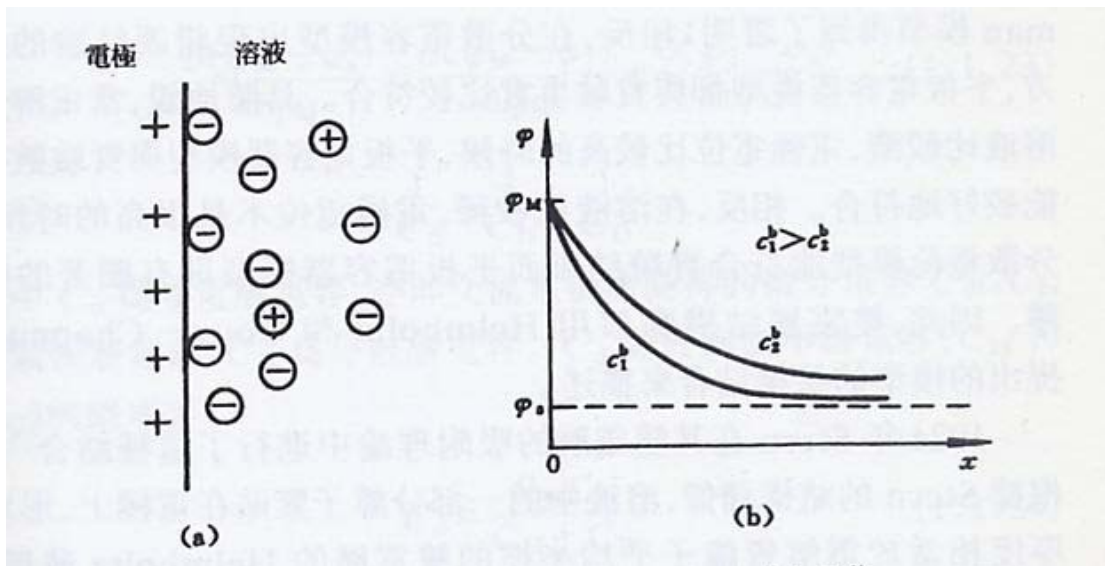


Figure 1-3 Schematic representation of Gouy and Chapman model

(a) The charge distribution (b) The potential distribution

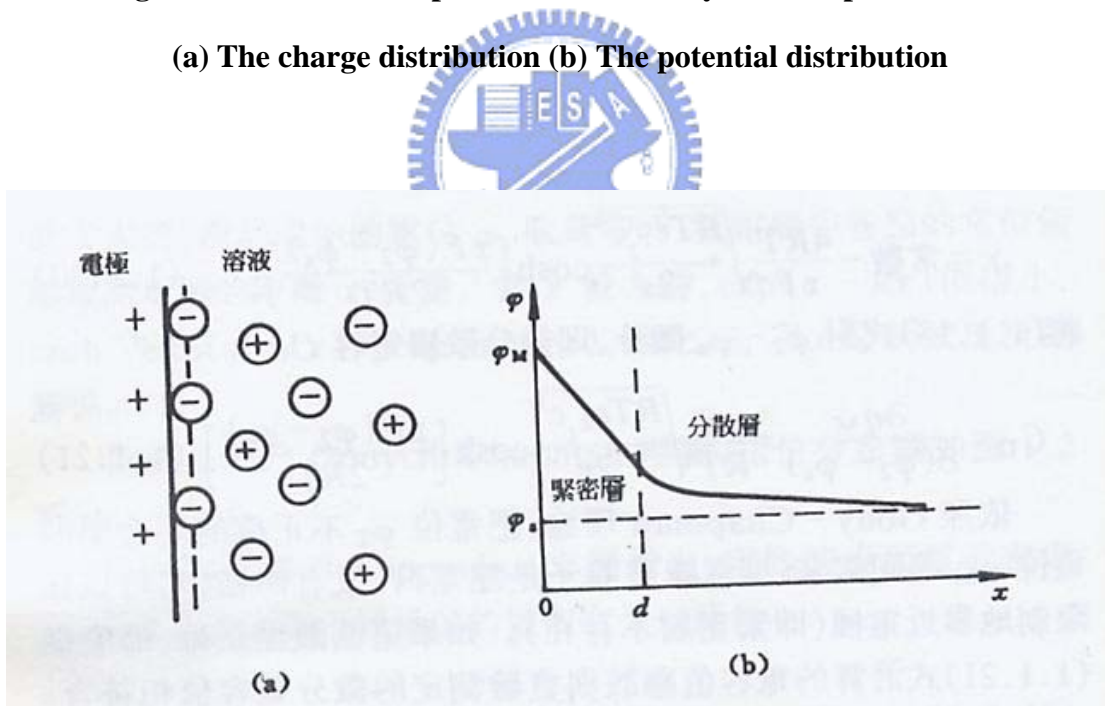


Figure 1-4 Schematic representation of Gouy – Chapman – Stern model

(a) The charge distribution (b) The potential distribution

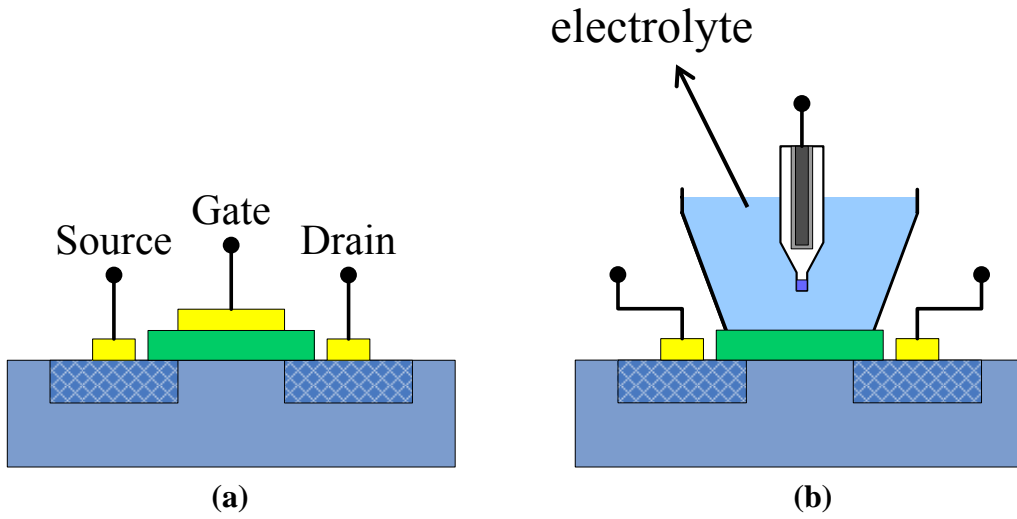


Figure 2-1 Schematic representation of (a) MOSFET, (b) ISFET

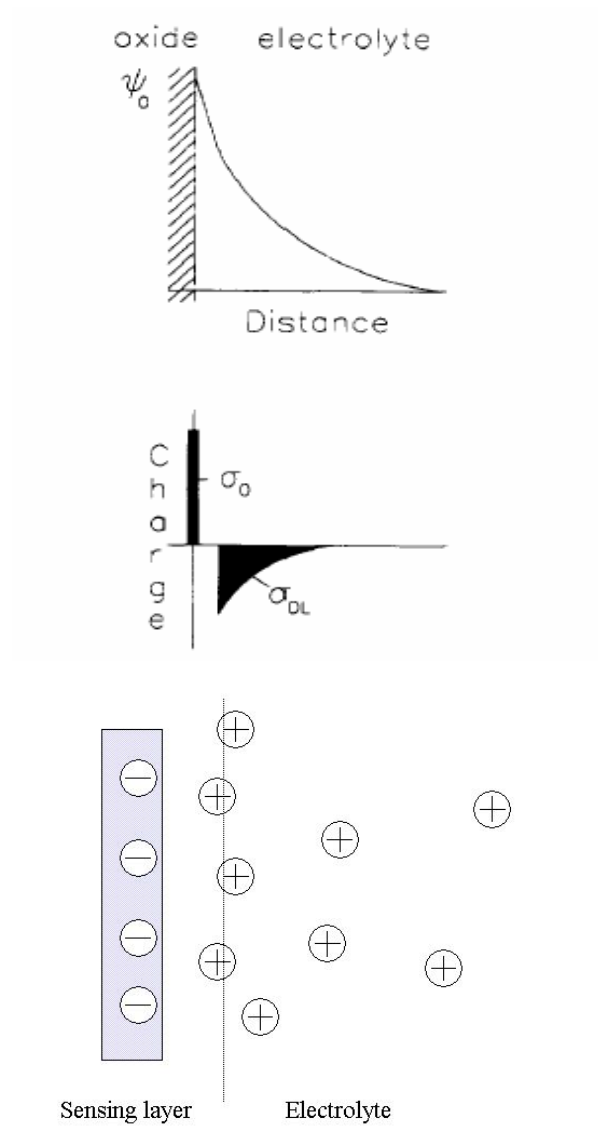


Figure 2-2 Potential profile and charge distribution at an oxide electrolyte solution interface

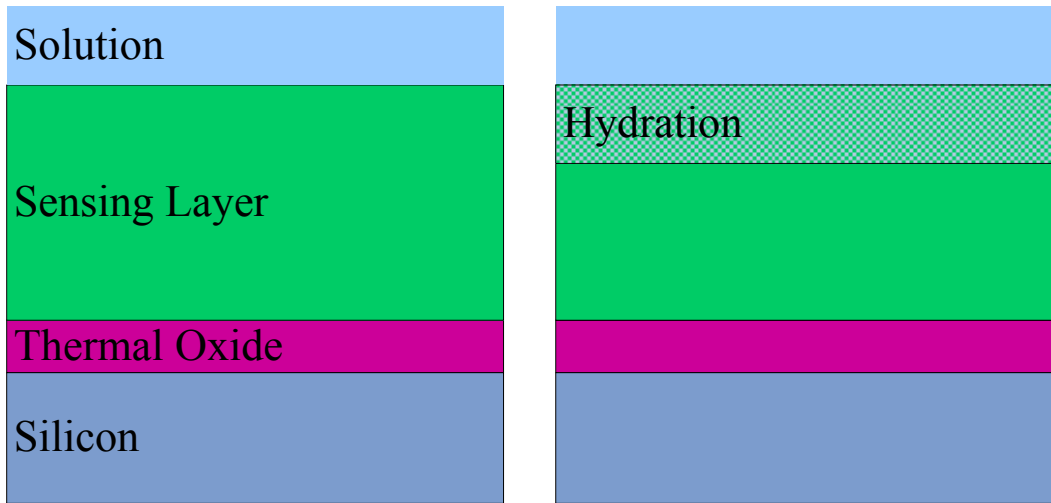
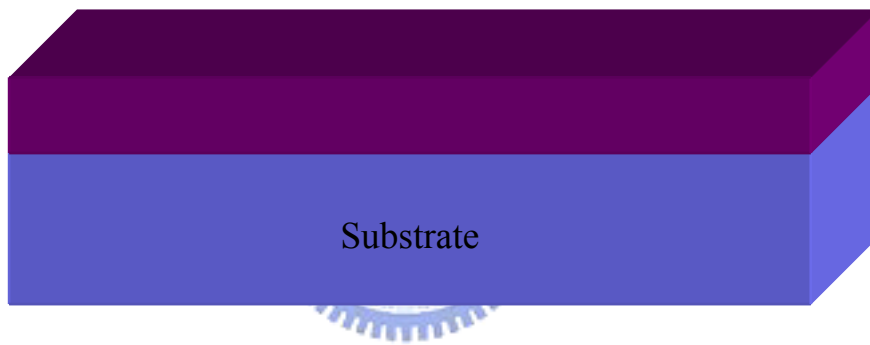
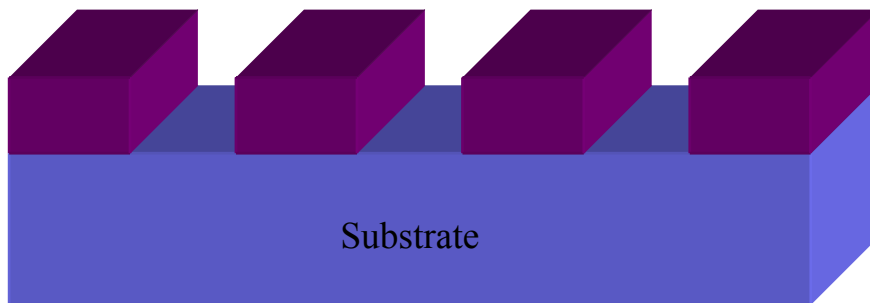


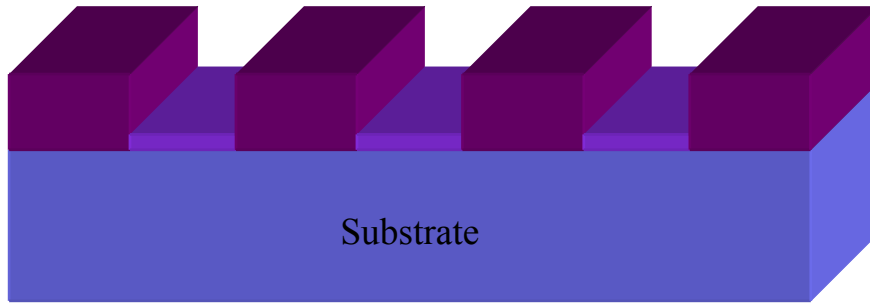
Figure 2-3 Series combination of the (a) initial (b) hydrated insulator capacitance



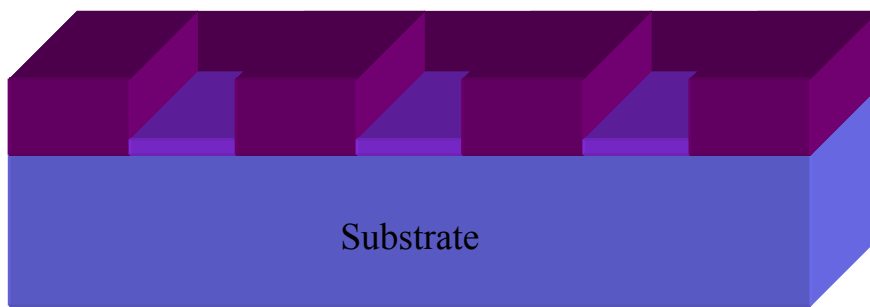
(a)



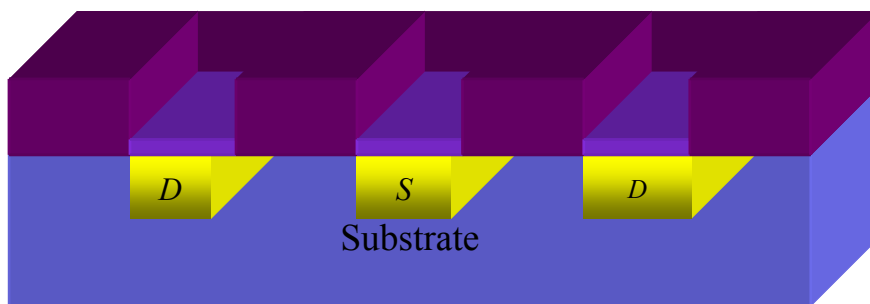
(b)



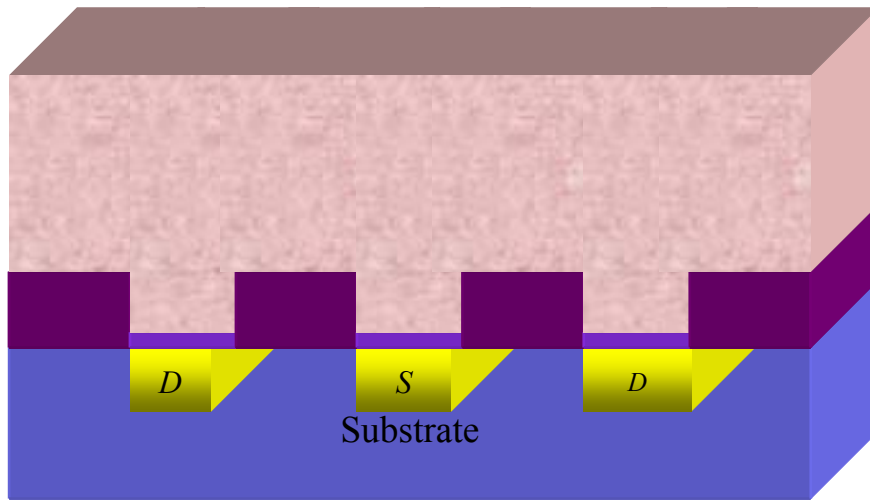
(c)



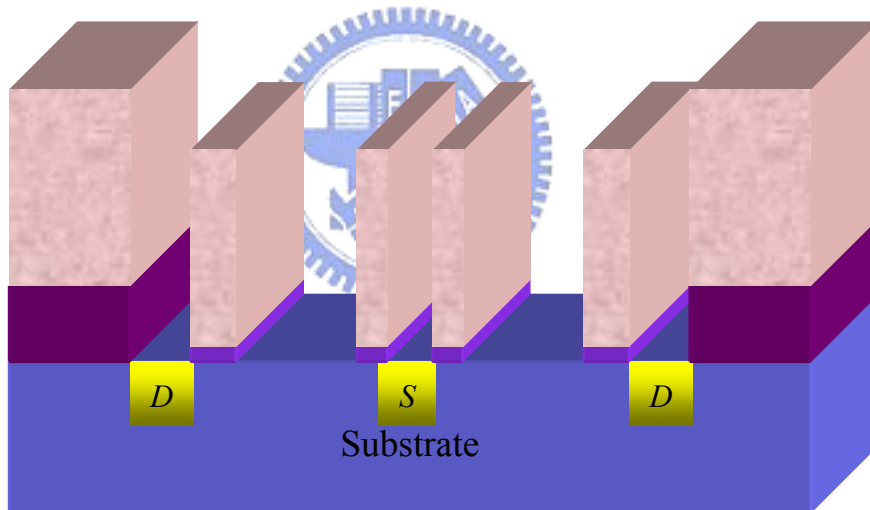
(d)



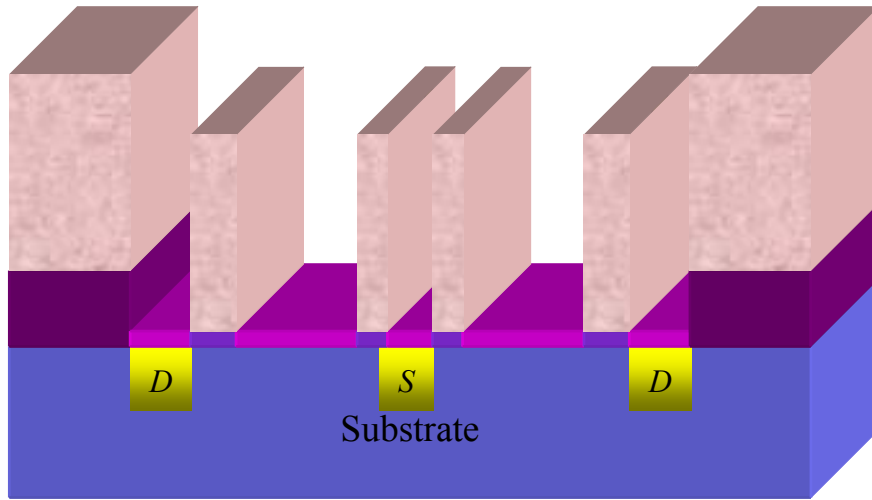
(e)



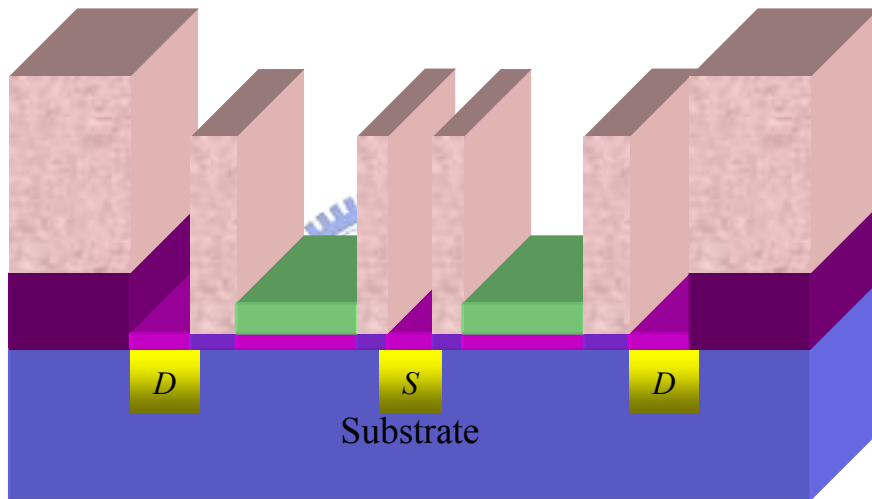
(f)



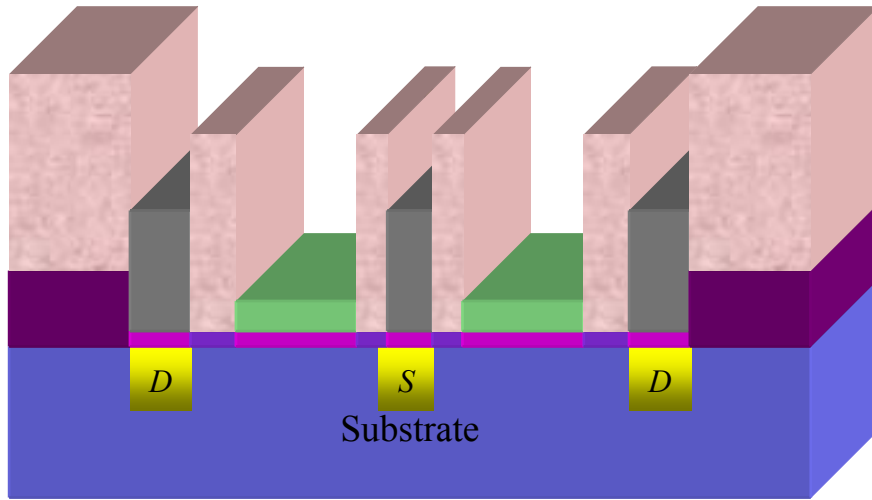
(g)



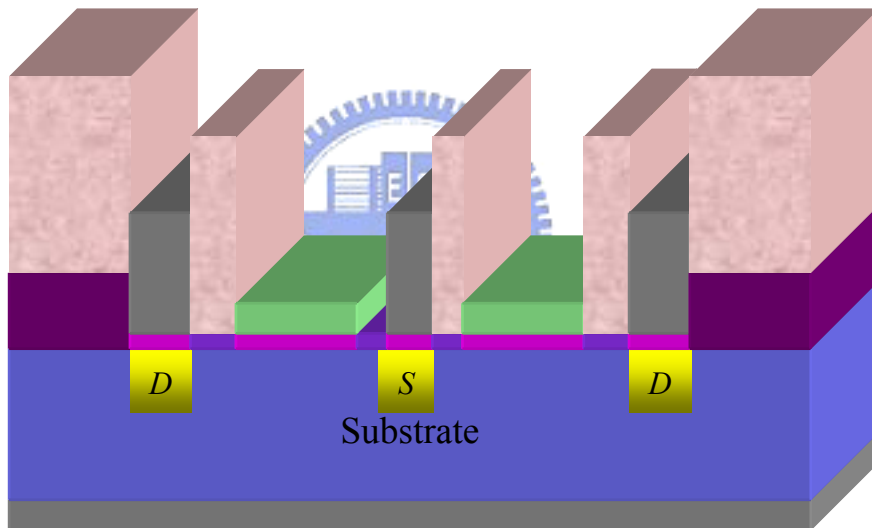
(h)



(i)



(j)



(k)

Figure 3-1 Fabrication process flow

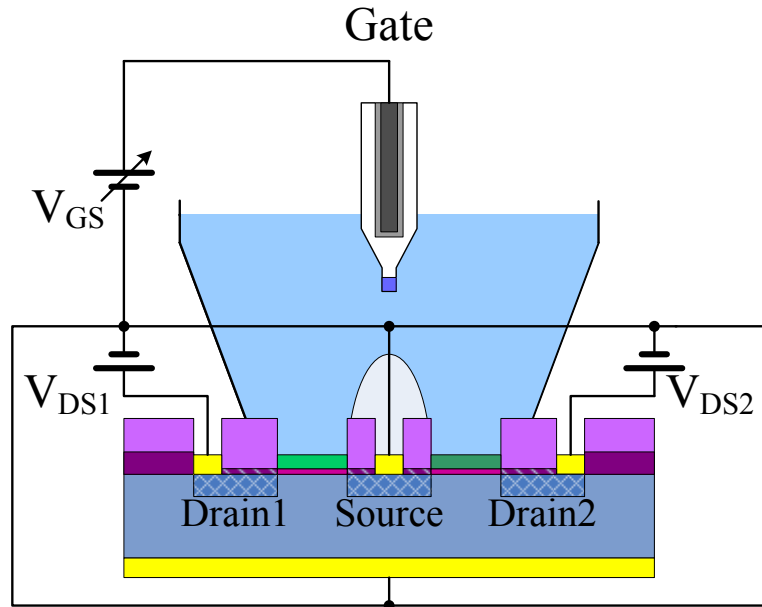


Figure 3-2 Measurement setup

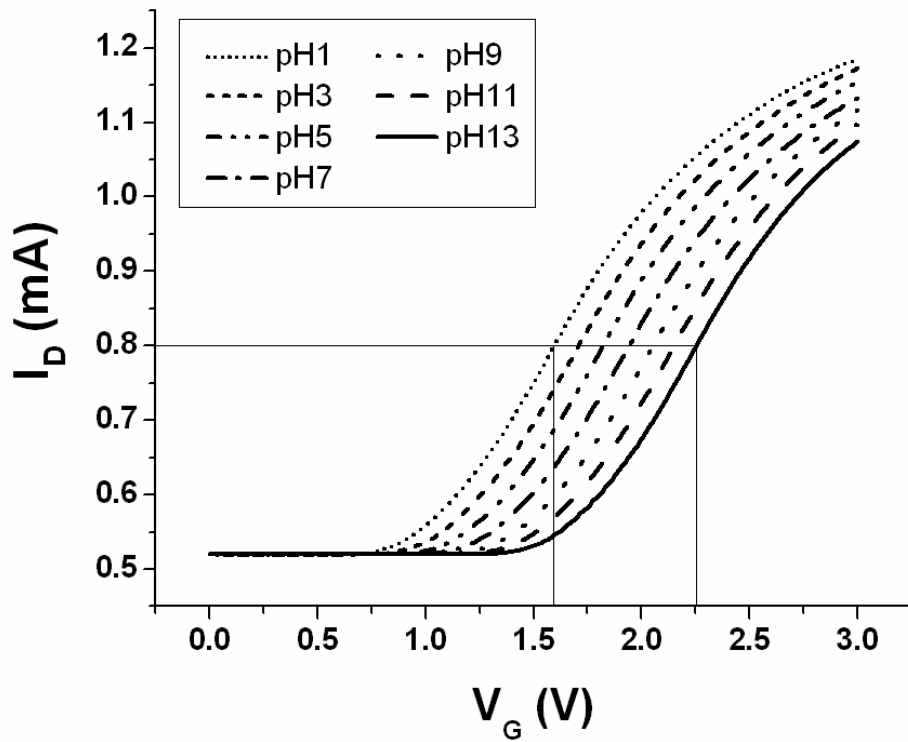


Figure 3-3 Detection principle of pH

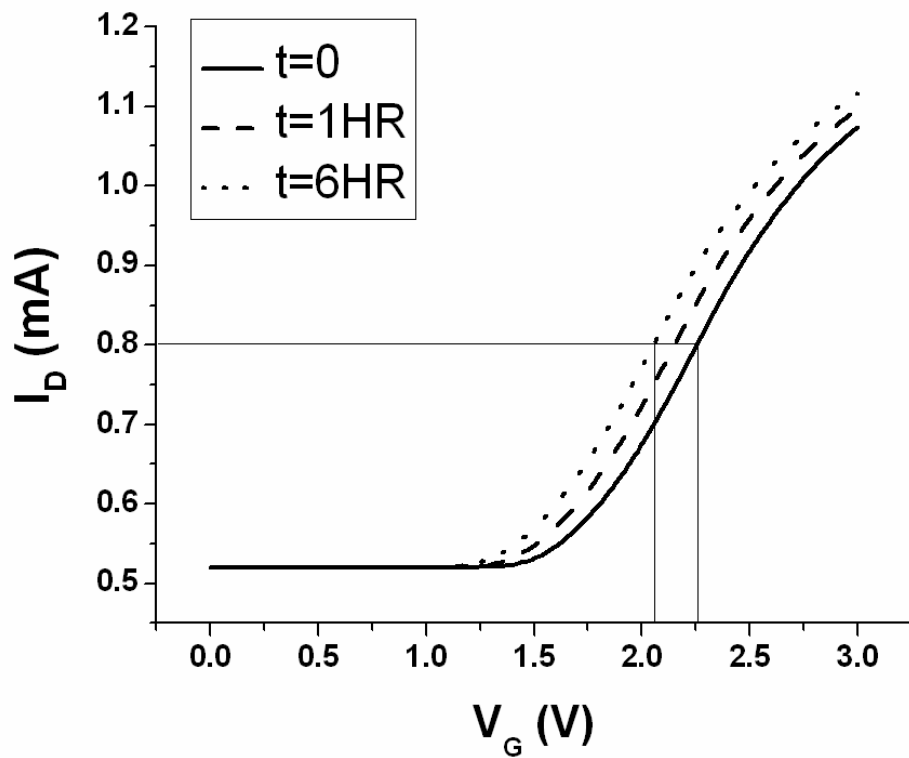


Figure 3-4 Detection principle of drift

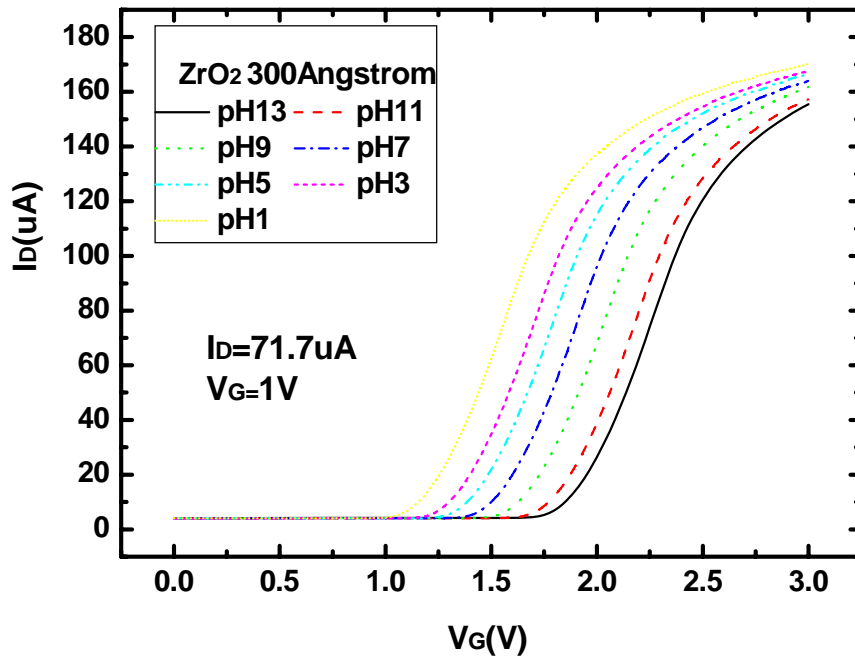


Figure 4-1 I_D - V_G curve of ZrO₂ to n-type ISFET before drift

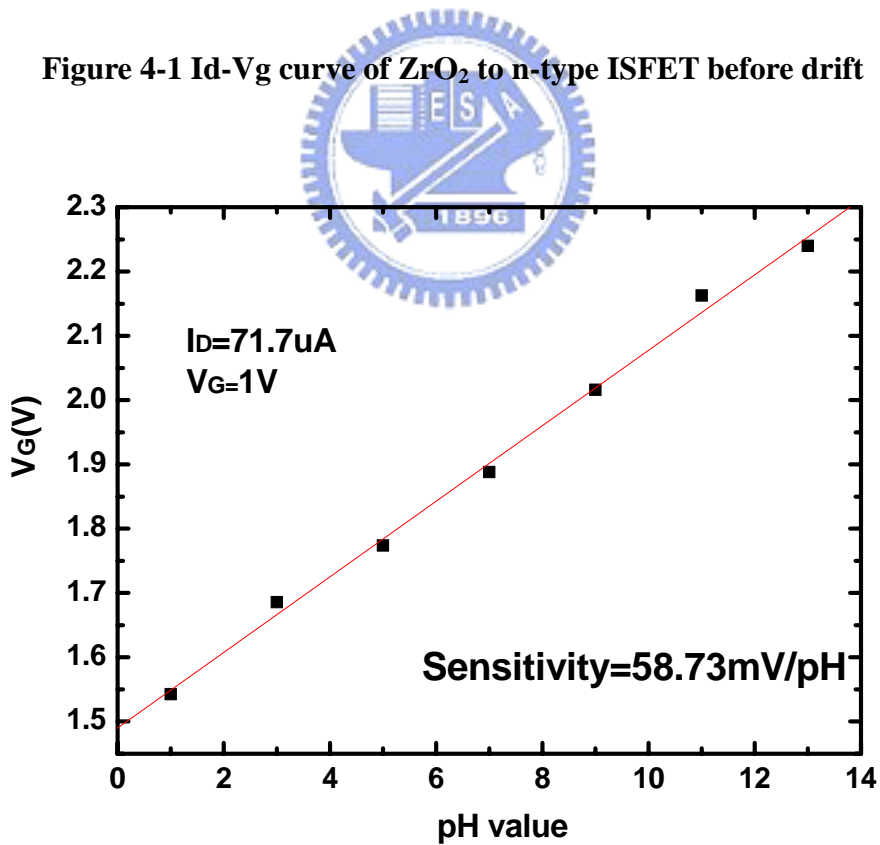


Figure 4-2 Sensitivity characteristic of ZrO₂ to n-type ISFET before drift

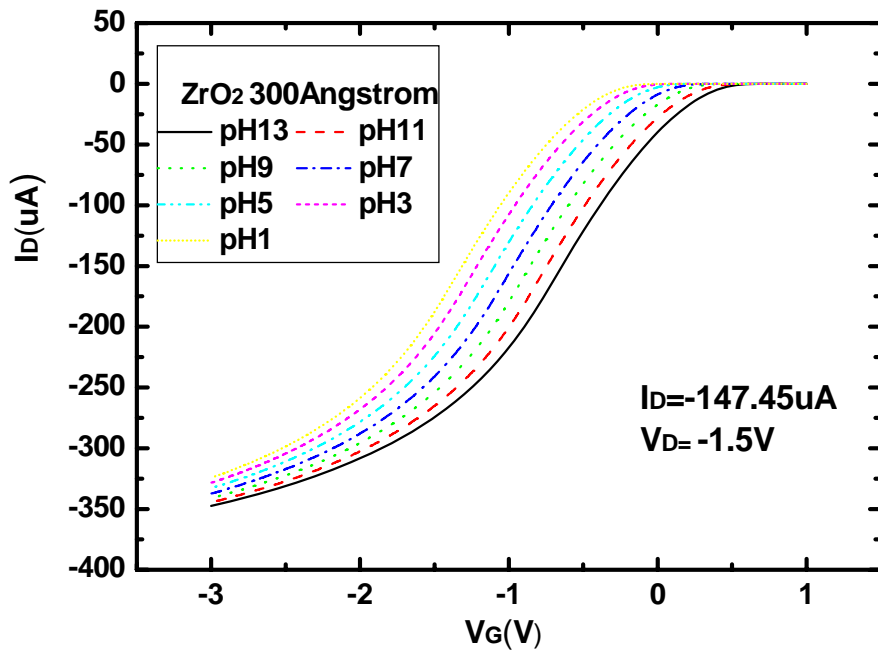


Figure 4-3 I_D - V_G curve of ZrO₂ to p-type ISFET before drift

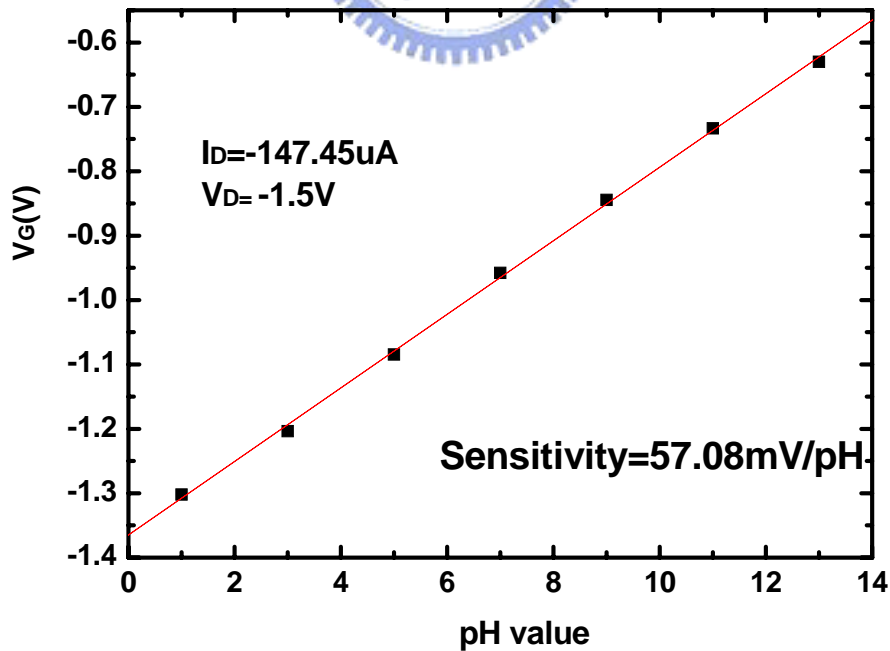


Figure 4-4 Sensitivity characteristic of ZrO₂ to p-type ISFET before drift

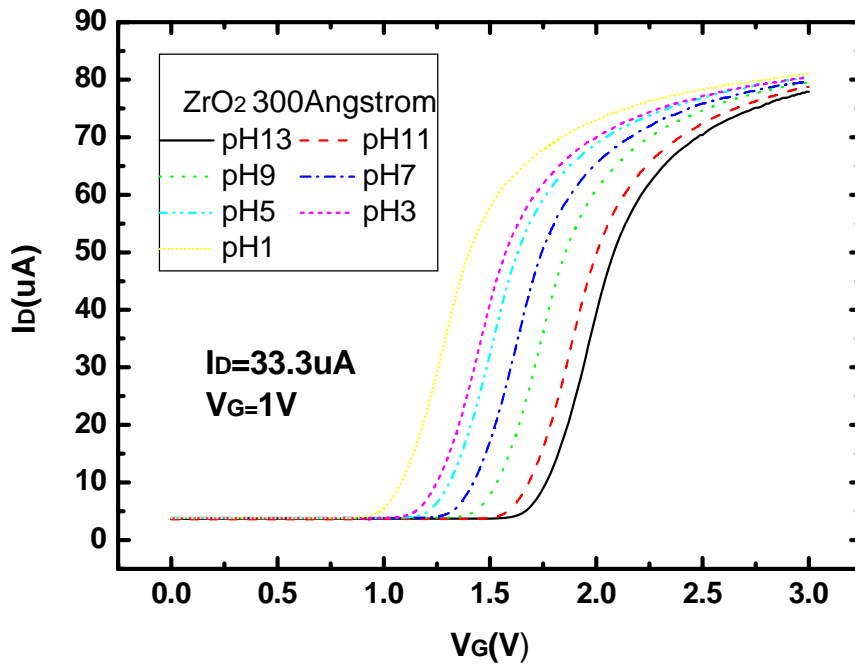


Figure 4-5 Id-V_g curve of ZrO₂ to n-type ISFET after drift in pH7 buffer solution for 7 hours

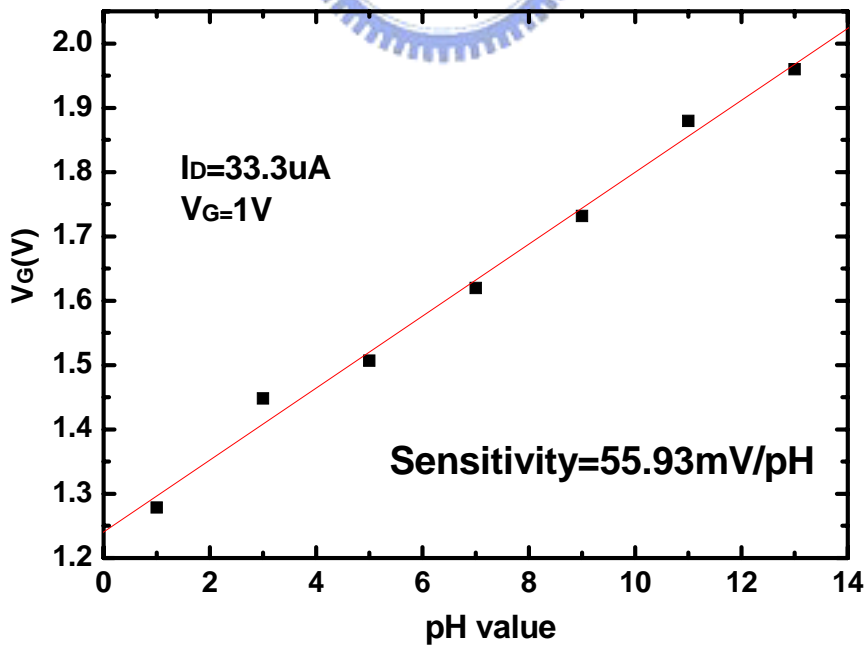


Figure 4-6 Sensitivity characteristic of ZrO₂ to n-type ISFET after drift in pH7 buffer solution for 7 hours

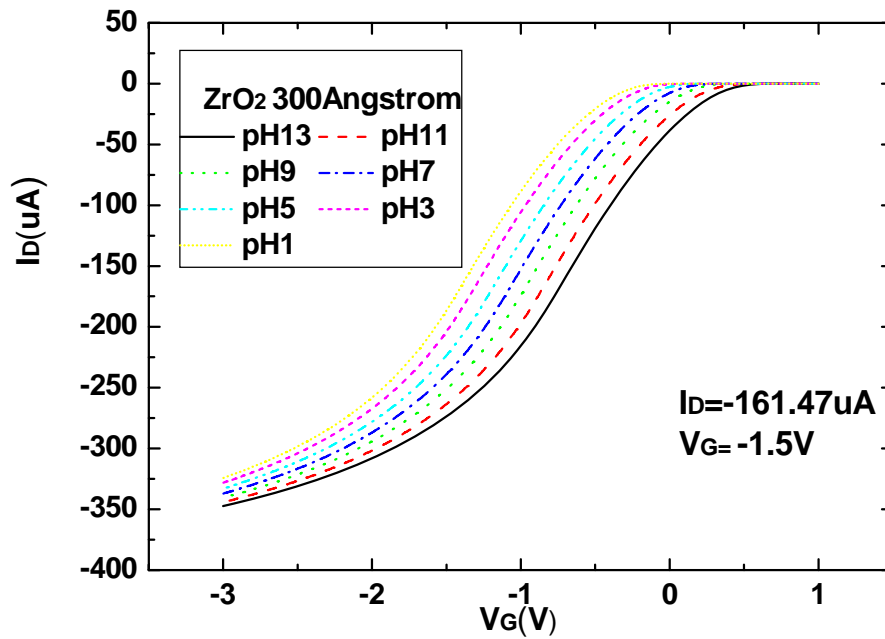


Figure 4-7 Id-Vg curve of ZrO₂ to p-type ISFET after drift in pH7 buffer solution for 7 hours

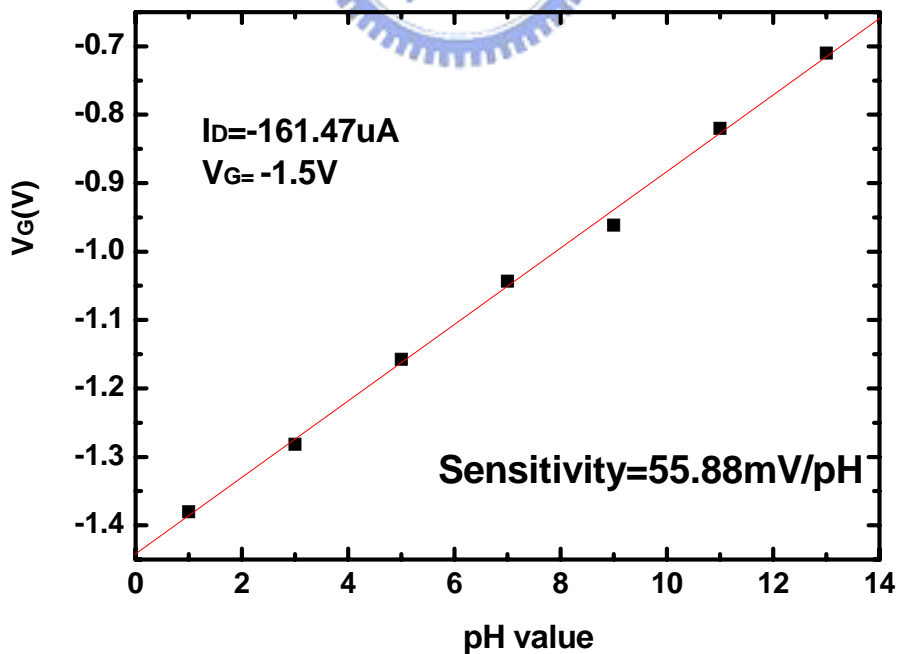


Figure 4-8 Sensitivity characteristic of ZrO₂ to p-type ISFET after drift in pH7 buffer solution for 7 hours

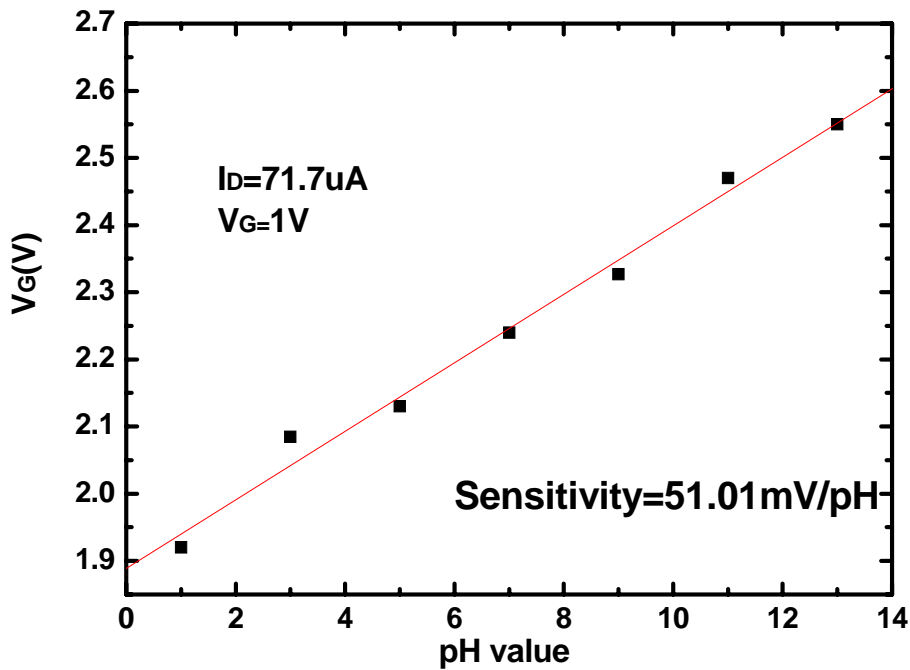


Figure 4-9 Sensitivity characteristic of ZrO_2 to n-type ISFET after drift in pH7 buffer solution 7 hours whose operation current is the same as original sensitivity

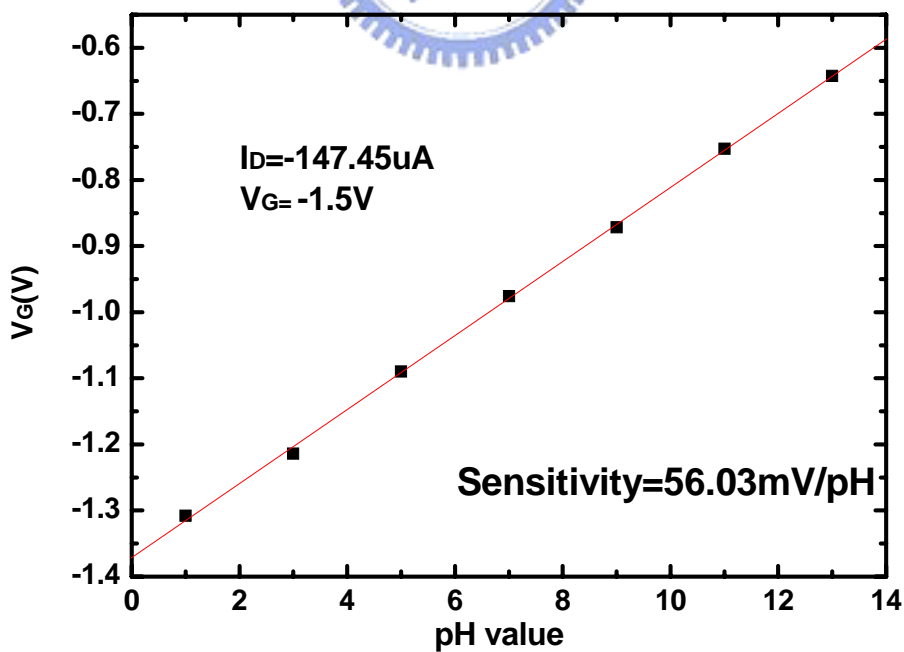


Figure 4-10 Sensitivity characteristic of ZrO_2 to p-type ISFET after drift in pH7 buffer solution 7 hours whose operation current is the same as original sensitivity

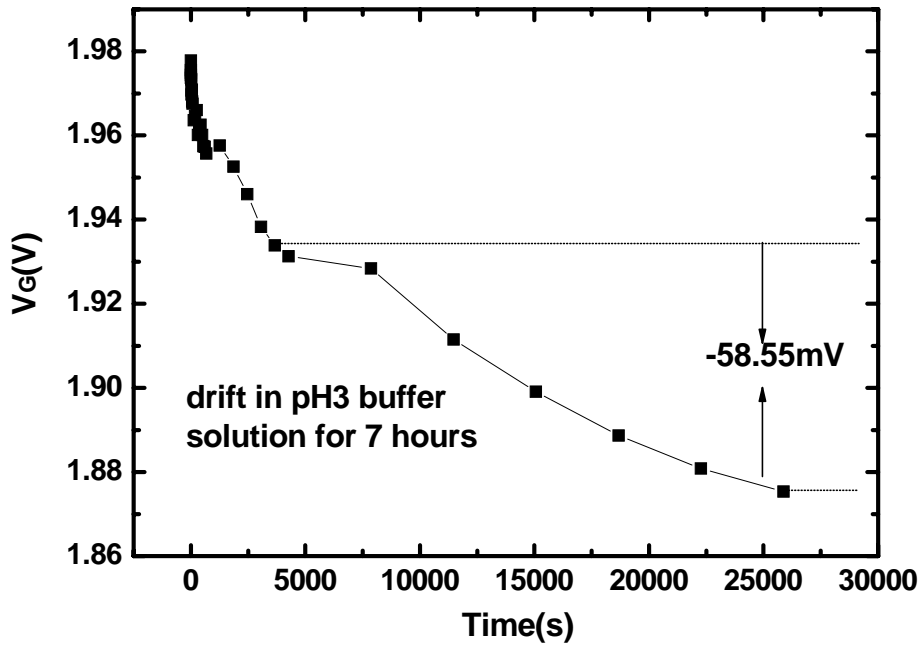


Figure 4-11 Time to drift in pH3 buffer solution of n-type ISFEET for 7 hours

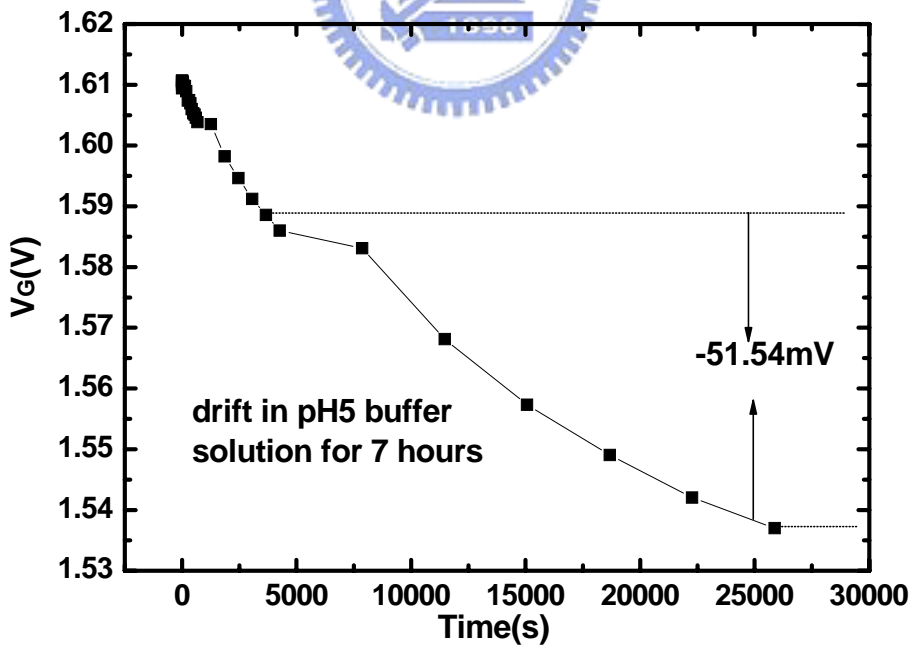


Figure 4-12 Time to drift in pH5 buffer solution of n-type ISFEET for 7 hours

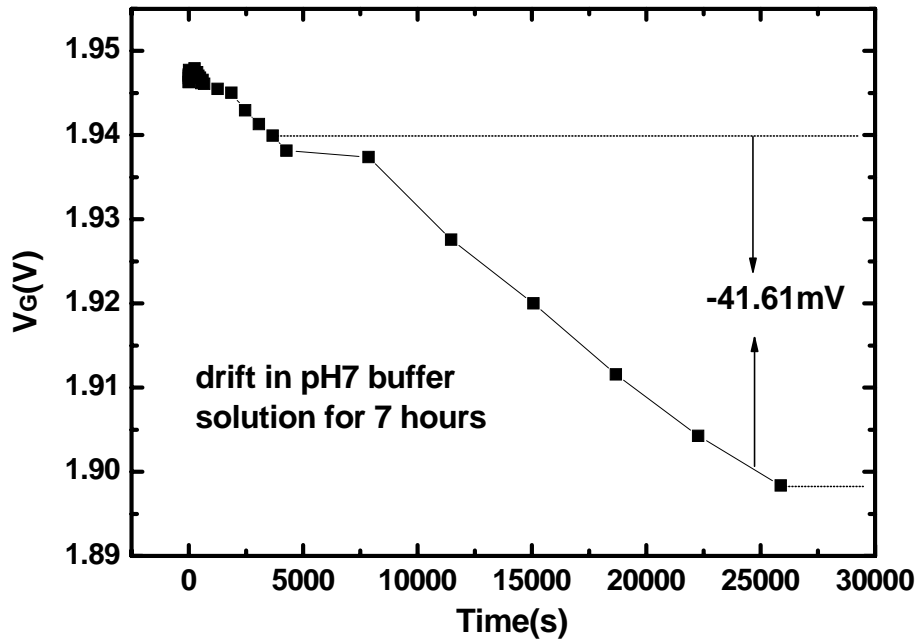


Figure 4-13 Time to drift in pH7 buffer solution of n-type ISFEET for 7 hours

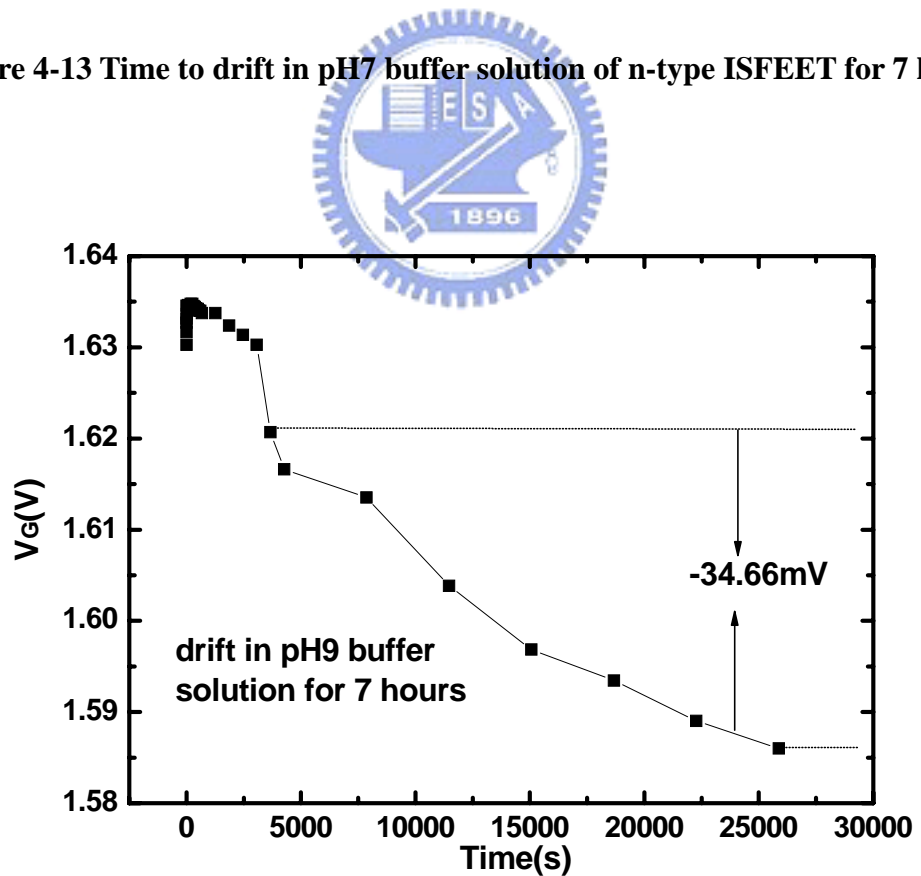


Figure 4-14 Time to drift in pH9 buffer solution of n-type ISFEET for 7 hours

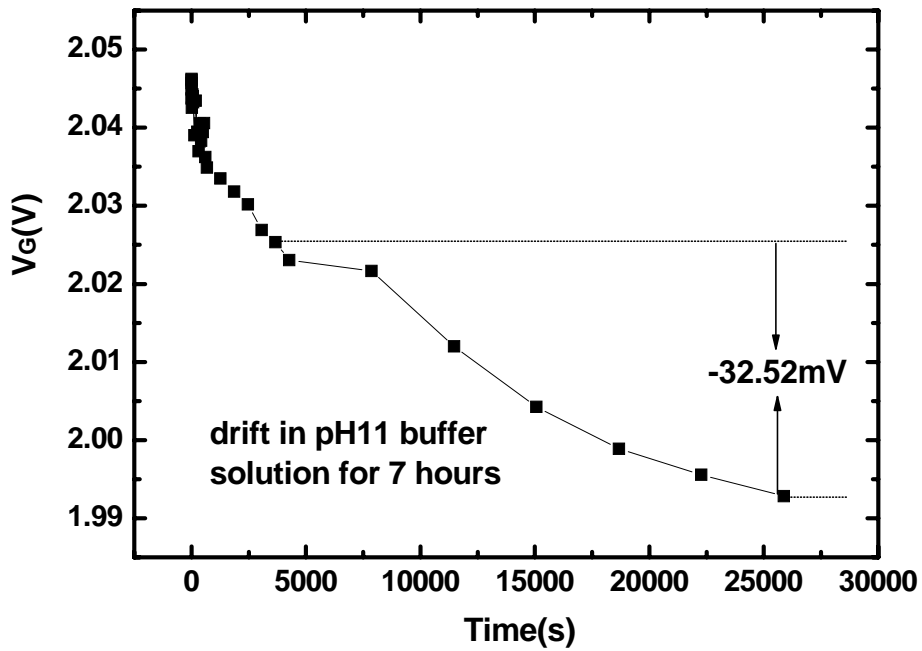


Figure 4-15 Time to drift in pH11 buffer solution of n-type ISFEET for 7 hours

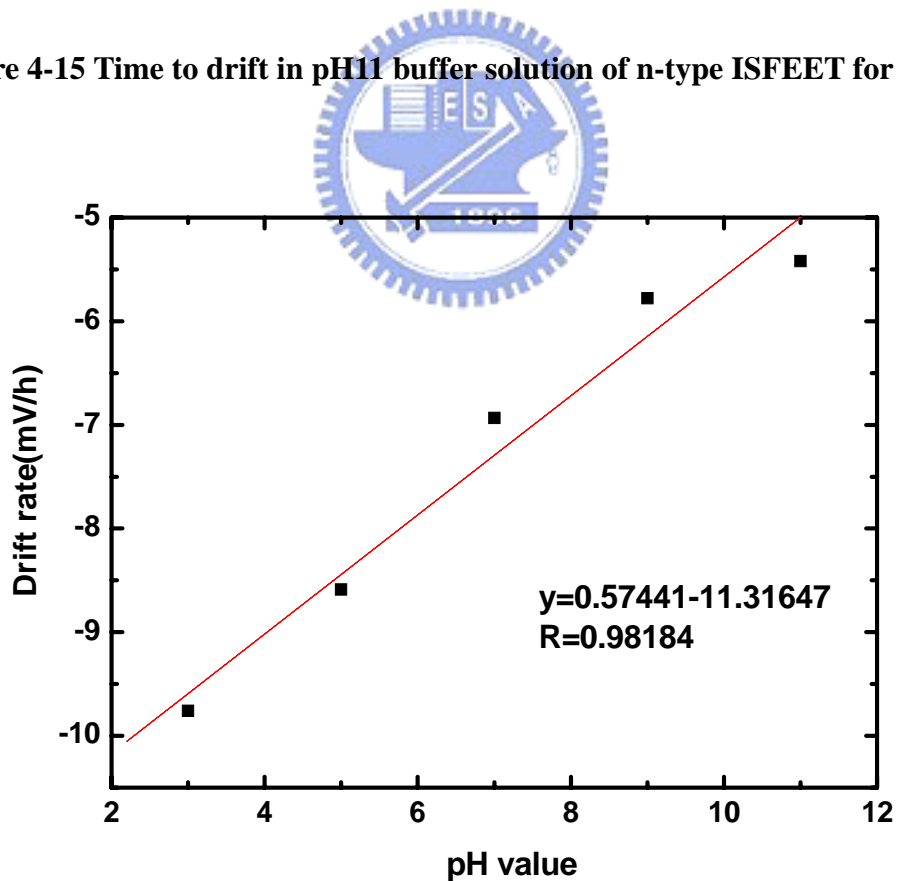


Figure 4-16 Time to drift rate of n-type ISFET in various buffer solution

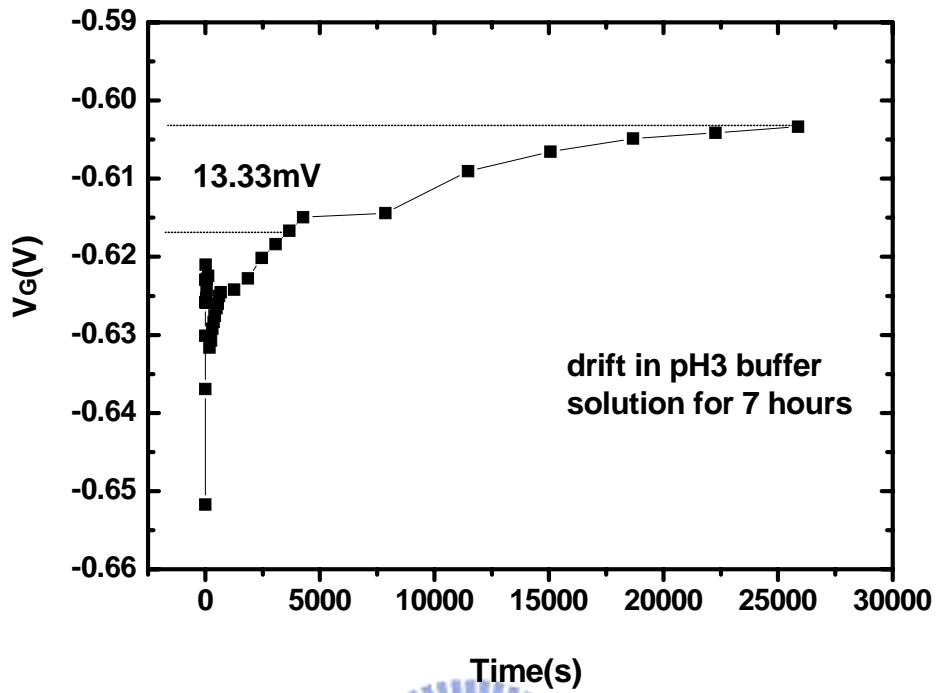


Figure 4-17 Time to drift in pH3 buffer solution of p-type ISFEET for 7 hours

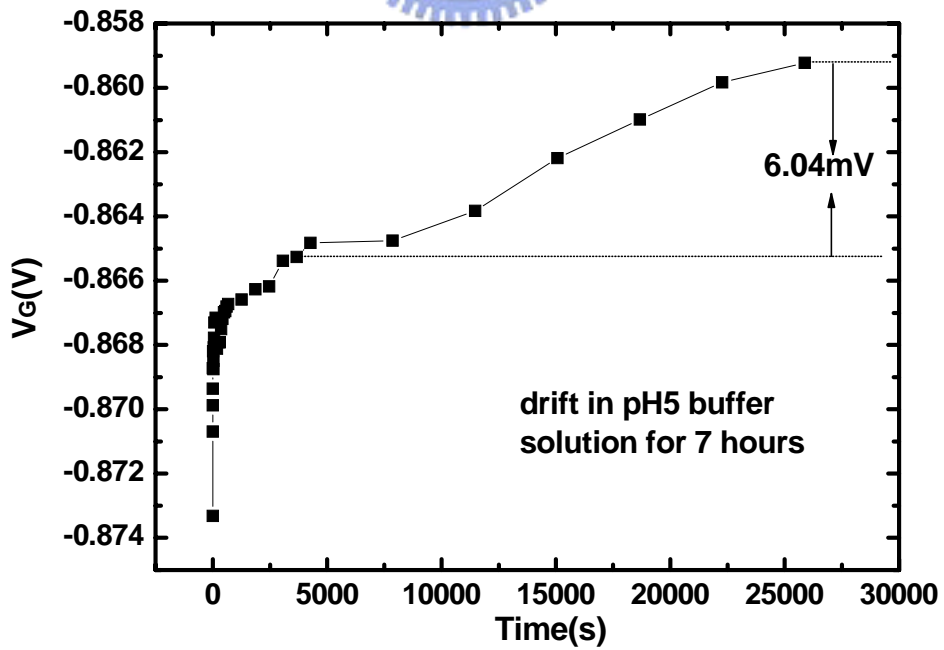


Figure 4-18 Time to drift in pH5 buffer solution of p-type ISFEET for 7 hours

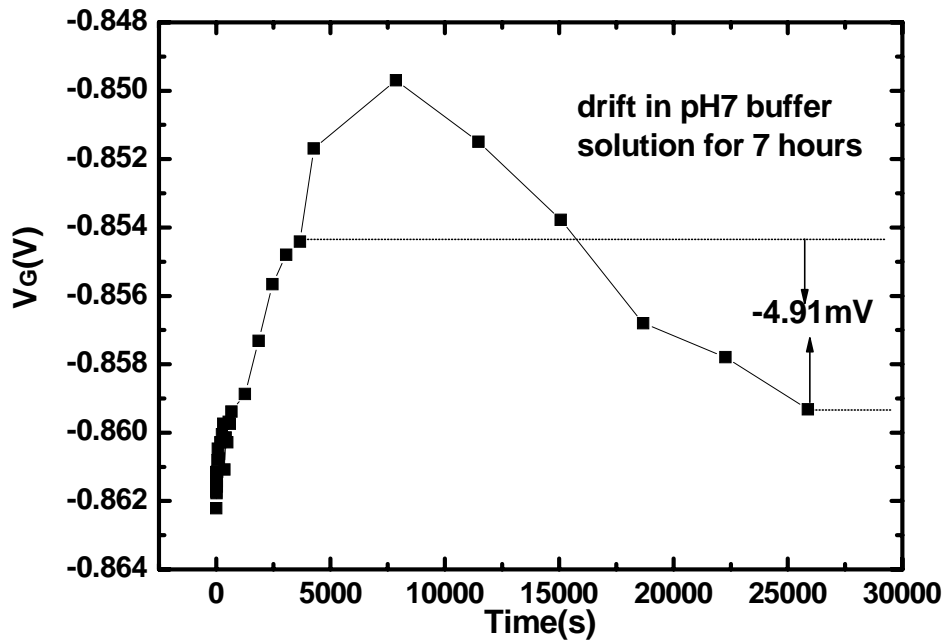


Figure 4-19 Time to drift in pH7 buffer solution of p-type ISFEET for 7 hours

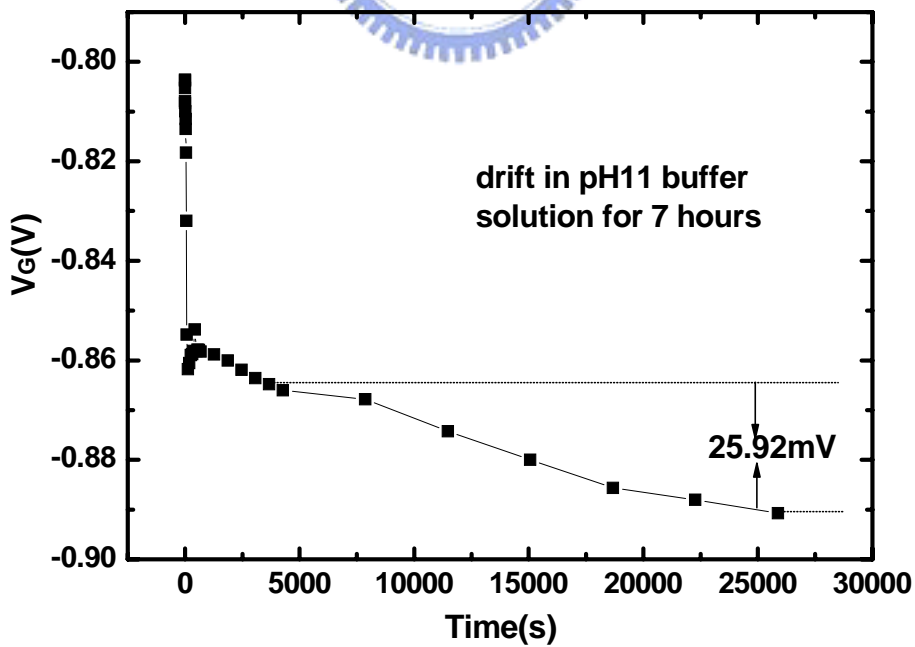
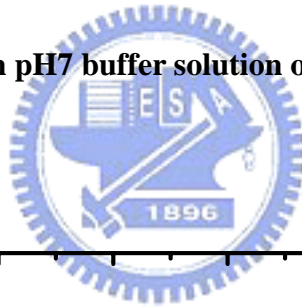


Figure 4-20 Time to drift in pH9 buffer solution of p-type ISFEET for 7 hours

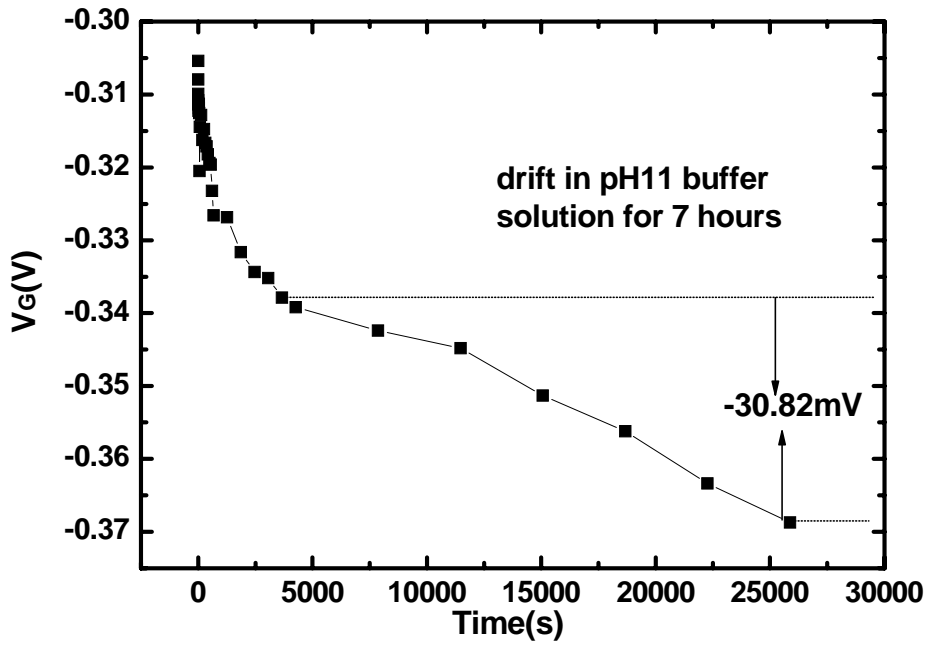


Figure 4-21 Time to drift in pH11 buffer solution of p-type ISFET for 7 hours

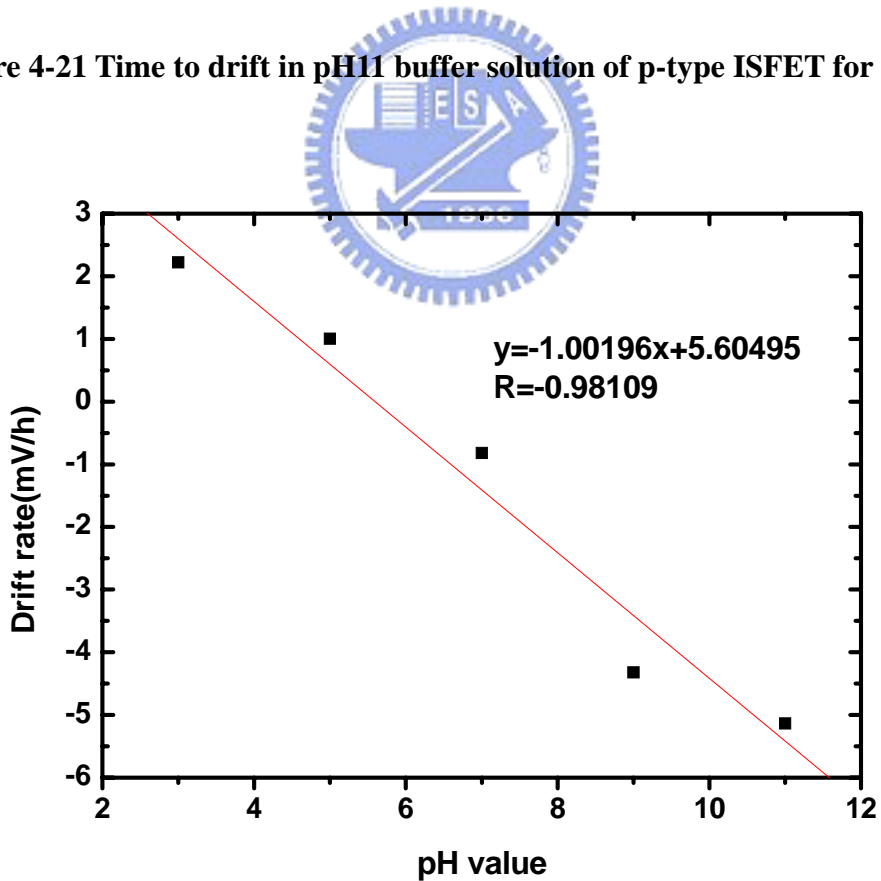


Figure 4-22 Time to drift rate of p-type ISFET in various buffer solution

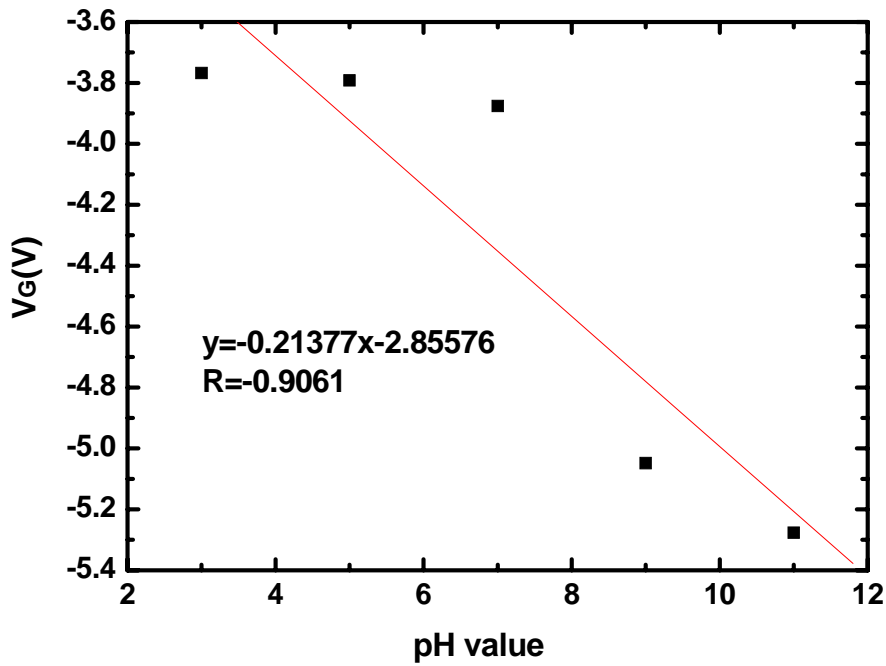


Figure 4-23 Time to drift of the compensation on the pH-ISFET in various buffer solution

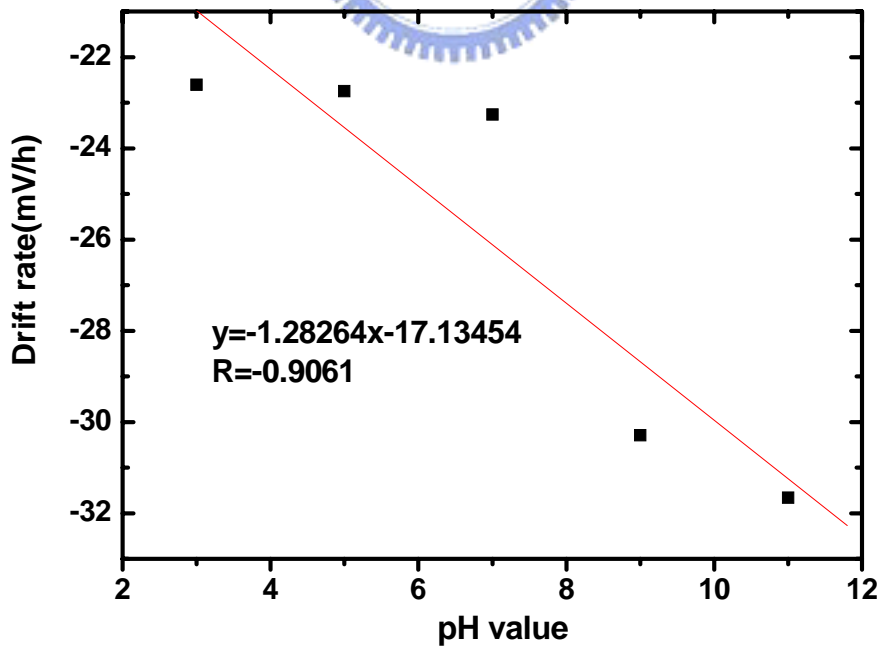


Figure 4-24 Time to drift rate of the compensation on the pH-ISFET in various buffer solution

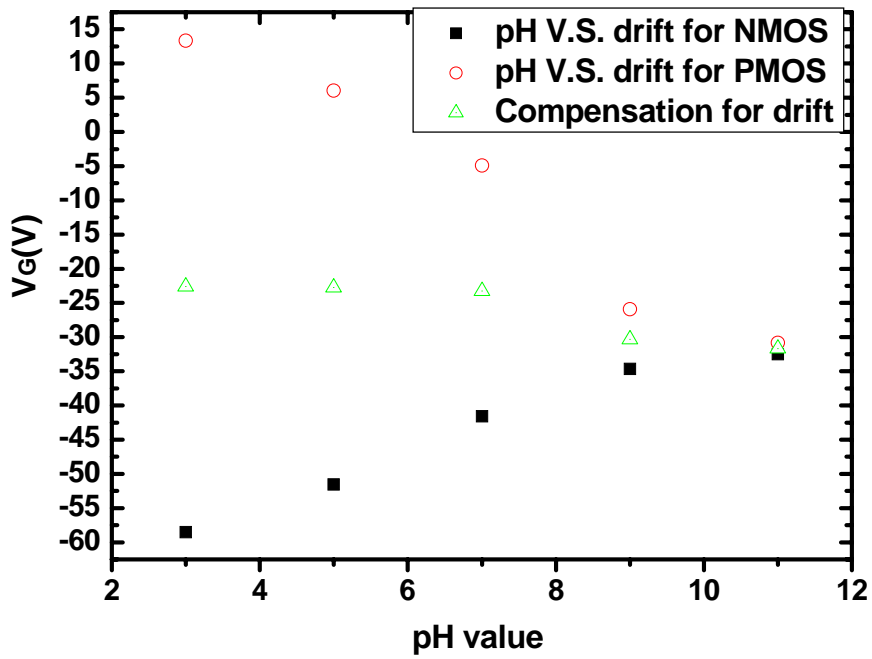


Figure 4-25 The comparison of drift between compensative drift and the original drift to the pH-ISFET in various buffer solution

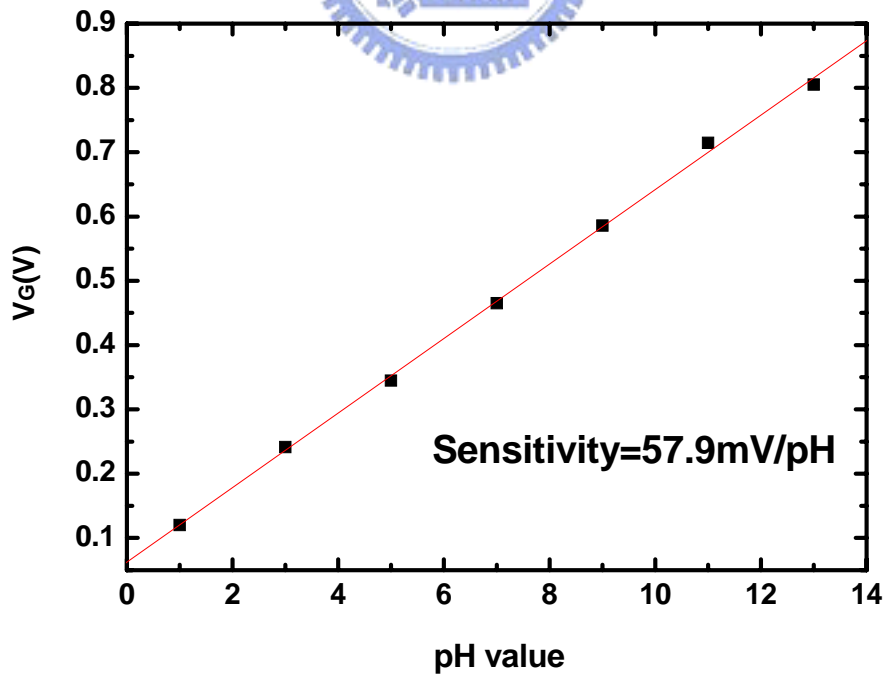


Figure 4-26 The comparison of sensitivity between compensative sensitivity and the original sensitivity to the pH-ISFET

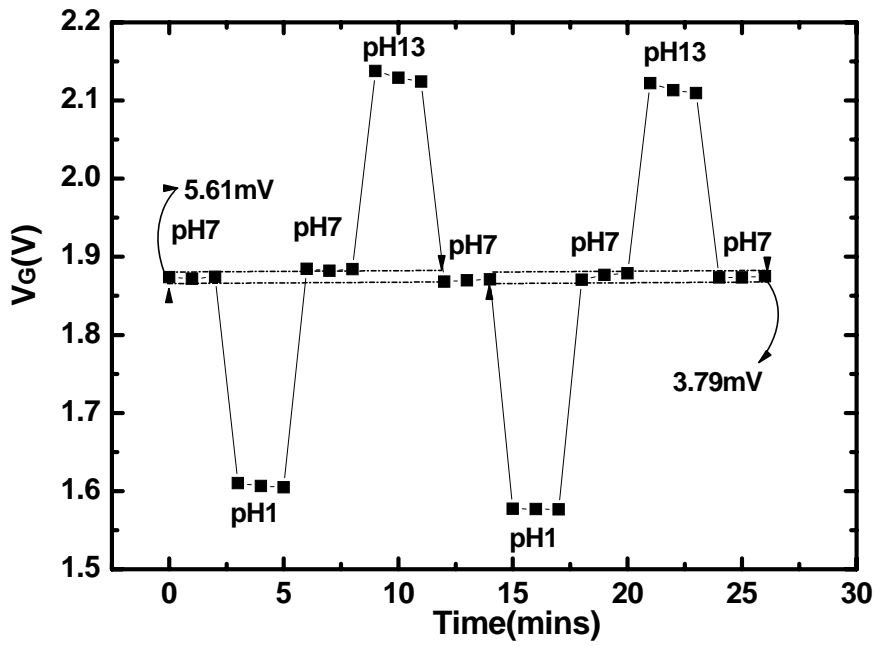


Figure 4-27 Hysteresis phenomenon to time of n-type pH-ISFET

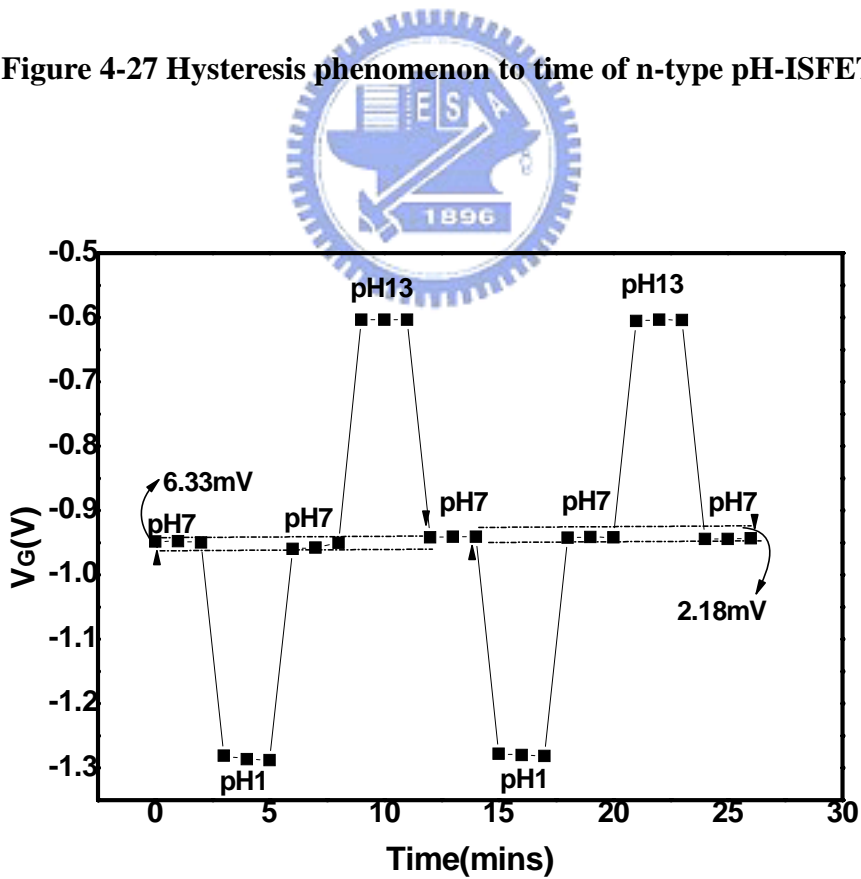


Figure 4-28 Hysteresis phenomenon to time of p-type pH-ISFET

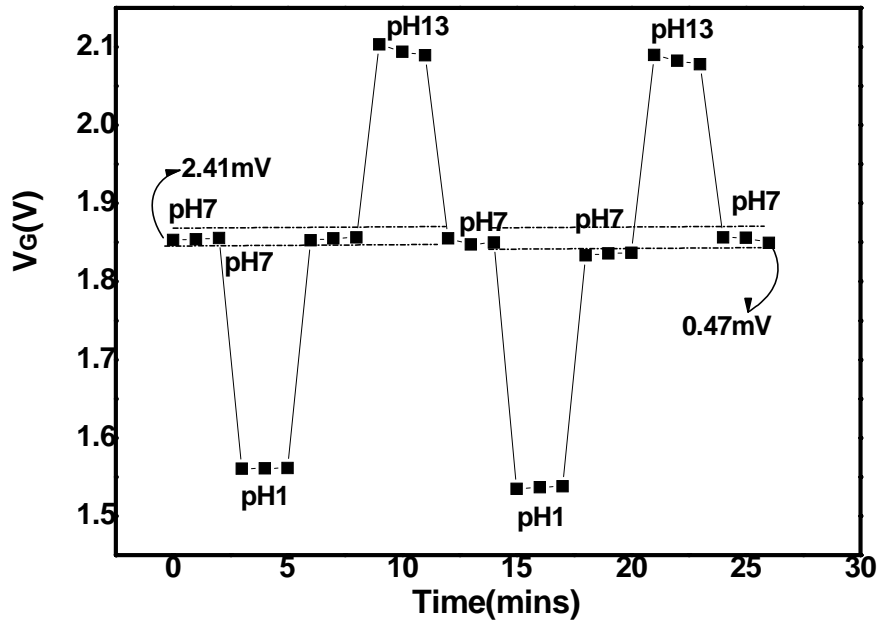


Figure 4-29 Hysteresis phenomenon to time of n-type pH-ISFET after drift in pH7 buffer solution for 7 hours

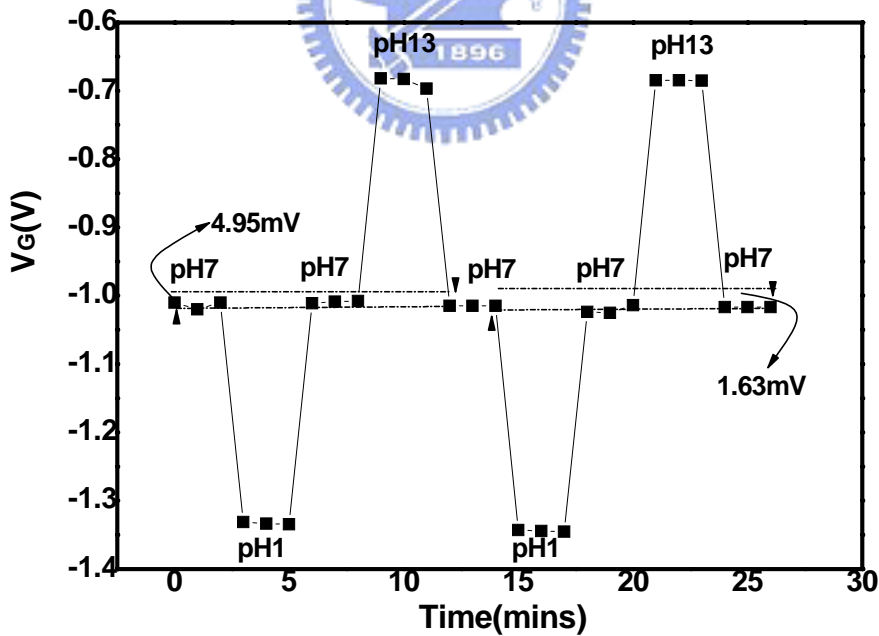


Figure 4-30 Hysteresis phenomenon to time of p-type pH-ISFET after drift in pH7 buffer solution for 7 hours

Diameter (mm): 100+/-0.5	Diameter (mm): 100+/-0.5
Type / Dopant : P / Boron	Type / Dopant : P / Phosphorous
Orientation : <100>	Orientation : <100>
Resistivity (ohm-cm):1-10	Resistivity (ohm-cm):1-12
Thickness (μ m) : 505-545	Thickness (μ m) : 515545
Grade : Prime	Grade : Prime

Table 3-1 (a) Specifications of wafers

parameters of ZrO₂ sputter
power : 200 W
Ar / O₂ : 24 / 8 (sccm)
Density : 6.51
Acoustic impedance : 14.72
Tooling factor : 0.533
Rate : 0.01 Å / s
pre sputter 60W for 10 min
Pressure : 7.6×10^{-3}

**Table 3-1 (b) Specifications of wafers
Parameters of sensing layers deposition with Sputter**

	N-type pH-ISFET	P-type pH-ISFET
Original sensitivity/ operation current	58.73mV/pH / 71.7 μ A	57.08 mV /pH / -147.45 μ A
Drifted sensitivity/ operation current	55.93 mV /pH / 33.3 μ A	55.88 mV /pH / -161.47 μ A

Table 4-1 Sensitivity at the optimum operation current

	N-type pH-ISFET	P-type pH-ISFET
Original sensitivity/ operation current	58.73 mV /pH / 71.7 μ A	57.08 mV /pH / -147.45 μ A
Drifted sensitivity/ operation current	51.01 mV /pH / 71.7 μ A	56.03m mV pH / -147.45 μ A

Table 4-2 Sensitivity at the immobile operation current

	N-type pH-ISFET	The compensation of pH-ISFET	P-type pH-ISFET
pH3	-58.55 mV	-22.61 mV	13.33 mV
pH5	-51.54 mV	-22.75 mV	6.04 mV
pH7	-41.61 mV	-23.26 mV	-4.91 mV
pH9	-34.66 mV	-30.29 mV	-25.92 mV
pH11	-32.52 mV	-31.66 mV	-30.82 mV

Table 4-3 Total drift in different pH buffer solution for 6 hours

	N-type pH-ISFET	The compensation of pH-ISFET	P-type pH-ISFET
pH3	-9.76 mV /h	-3.77 mV /h	2.22 mV /h
pH5	-8.59 mV /h	-3.79 mV /h	1.01 mV /h
pH7	-6.94 mV /h	-3.88 mV /h	-0.82 mV /h
pH9	-5.78 mV /h	-5.05 mV /h	-4.32 mV /h
pH11	-5.42 mV /h	-5.28 mV /h	-5.14 mV /h

Table 4-4 Drift rate in different pH buffer solution for 6 hours

	N-type pH-ISFET	The compensation of pH-ISFET	P-type pH-ISFET
Sensitivity	58.73 mV/pH	57.9 mV/pH	57.08 mV/pH

Table 4-5 The comparison of the sensitivity

	N-type pH-ISFET before drift	N-type pH-ISFET after drift	P-type pH-ISFET before drift	P-type pH-ISFET after drift
1st cycle	5.61mV (0.095pH)	2.41 mV (0.043pH)	6.66 mV (0.111pH)	4.95 mV (0.089pH)
2nd cycle	3.79 mV (0.064pH)	0.47 mV (0.008pH)	2.18 mV (0.038pH)	1.63 mV (0.029pH)

Table 4-6 The comparison of the sensitivity

個人簡歷

姓名：林佳鴻

性別：男

生日：民國 71 年 1 月 10 日

籍貫：台灣省台中市

學歷：私立淡江大學電機工程學系 (89.9-94.6)

國立交通大學電子工程研究所 (94.9-96.7)

碩士論文題目：

二氧化鋯感測層在 N 型及 P 型 pH-離子感測場效電晶體上之
研究與比較



**The study and comparison of ZrO₂ sensing film based on
N-type and P-type pH-ISFETs**